THE INSULATED GATE FIELD EFFECT TRANSISTOR (IGFET) AS A MICROLUMINOMETER

by

Robert S. Smith

Dissertation submitted to the Faculty of the
Virginia Polytechnic Institute and State University
in partial fulfillment of the requirements for the degree of

DOCTOR OF PHILOSOPHY

in

Chemistry

Approved:

Raymond E. Dessy, Chairman

John G. Mason

James P. Wightman

Brian E. Hanson

Mark R. Anderson

July, 1991

Blacksburg, Virginia

THE INSULATED GATE FIELD EFFECT TRANSISTOR (IGFET) AS A MICROLUMINOMETER

by

Robert S. Smith

Committee Chairman: Raymond E. Dessy
Chemistry

(ABSTRACT)

This work presents data concerning the optical nature of the insulated gate field effect transistor (IGFET), how its optical sensitivity relates to its electrical operation, and explores its usefulness as a microluminometer for a chemisensor and biosensor. Although the experiments performed for this dissertation show that the IGFET's light sensitivity does not involve the standard operation of the FET, i.e., the modulation of the source to drain current, they also show that the IGFET's light sensitivity is not a simple photodiode response of the source/base or drain/base junction. This work raises many interesting questions to be answered by future studies concerning the light sensitivity of the IGFET and its possible uses.

In this work an instrument was built to probe the IGFET with photons, the IGFET's wavelength response is presented, the detection of recaequorin in a static system is shown to have a limit of detection of $6*10^{-20}$ moles of recaequorin, and the IGFET is demonstrated as a microluminometer in a FIA system for detecting hypochlorite. The hypochlorite limit of detection is $39 * 10^{-12}$ moles..

The author proposes new uses for the IGFET employing its traditional ion sensing role as well as its photosensitivity. Construction of a three dimensional biosensor is suggested.

FOUR GENERATIONS OF SUPPORT

Helga and Rachael

RC

Daneta

Eric

ACKNOWLEDGMENTS

I thank Dr. and Mrs. Dessy for giving me the opportunity to pursue graduate work in their family, for their encouragement and guidance while I've been here, and for the strong support during the hunt for a faculty position. I thank the members of the chemistry faculty who have served on my committee. They have given warm support and encouragement and I could not go wrong emulating any of their teaching styles. I thank the Chemistry department for their financial support and giving me the opportunity to T.A. for Dr. Mason in analytical chemistry and advise students in LASC and GASC. This direct contact with students has helped me make the decision to pursue a teaching career. It was a pleasure to work with Deans Ogliaruso and Barnett and Drs. Creamer, Lane, and Owen and special thanks are extended to Barbara Wilkes for her persevering support during our five years together in the advising center.

Dr. Elshabini Riad, Monty Hayes, and Scott Massie have graciously shared their time and facilities in Electrical Engineering supporting this work. Mr. VanDamme built the world class glass flow cell. The electronic shop willingly loaned equipment to support this work and Jim Hall, Larry Jackson, Dave McCommon, and Jim Coulter patiently answered all my questions. Dr. Wightman and Frank Comer provided the surface study for this work.

Dr. Steve Caras provided the initial introduction to IGFET's during the two times I visited him at the Naval Research Labs. Dr. Jim Griffiths at NRL provided the highly fluorinated monomer and crosslinking agent. Kevin Ely at ITT provided logistic support and loaned equipment to help develop the early momentum of the project. Dr.

David Smith of the Biochemistry Department at the University of Georgia provided the recaequorin.

One of the most enjoyable aspects of my graduate education has been the introduction and exposure to machining that the physics shop machinists Fred Blair, Dave Miller, John Miller, Bob Ross, and Melvin Shaver provided. Last but not least it has been most enjoyable working and playing with the past and present members of the Dessy research group.

TABLE OF CONTENTS

LIST OF FIGURES

LIST OF TABLES

1. INTRODUCTION

This dissertation describes studies performed to characterize the insulated gate field effect transistor (IGFET) as a microluminometer. The IGFET was developed by Bergveld as an ion sensor (1). This work is the result of pursuing a fortuitous observation made while working with insulated gate field effect transistors (IGFET's), i.e., the unexpected observation that they are sensitive to light. The author's ion sensing IGFET instrument was constructed with a flow cell of clear epoxy and glass, with a Plexiglass shield, which combined, allowed ambient photons to strike the chip causing what at first appeared to be noise based on ambient light level. After this noise was evaluated and determined to result from light response, some preliminary experiments were run to determine the approximate level of sensitivity to light from a bioluminescent reaction. The author consulted Dr. Aicha Elshabini Riad, Professor of Electrical Engineering at Virginia Polytechnic Institute and State University, an expert in optical devices. She gave assurance that this device was worth characterizing as an optical sensor. This work presents data concerning the optical nature of this device, how its optical sensitivity relates to its electrical operation, and explores its usefulness as a microluminometer for a chemisensor and biosensor. Although the experiments performed for this dissertation show that the IGFET's light sensitivity does not involve the standard operation of the FET, i.e., the modulation of the source to drain current, they also show that the IGFET's light sensitivity is not a simple photodiode response of the source/base or drain/base junction. This work raises many interesting questions to

be answered with future studies concerning the light sensitivity of the IGFET and its possible uses.

The chips used were provided by Dr. Jiri Janata, Professor of Biomedical Engineering at the University of Utah. They are mounted on a 1.28mm x 2.16mm die shown in Figure 1, containing four transistors; two MOSFETs and two IGFETs as shown in Figure 2. One of the IGFET's drain, gate, and source are labeled in Figure 3. The source and drain areas are silicon doped with phosphorous. Phosphorous atoms are introduced into the surface of the silicon either by ion implantation or chemical diffusion. The top layer of the gate is about 1000 angstroms of silicon nitride. Silicon nitride is typically grown by chemical vapour deposition at 600-800°C in a nitrogen atmosphere containing ammonia and silane. The gate dimension is 20 x 400 microns. The pads and runners for making wirebond connection to the chip and connection to the source and drain are aluminum. These are made by etching holes through the insulator surface (field nitride) and evaporating aluminum on the surface. A side view, not to scale, of a metal oxide semiconductor field effect transistor, MOSFET, is shown in Figure 4. For the IGFET the metal layer at the gate is not present. The insulation layer is about 1000 angstroms of silicon nitride on top of about 1000 angstroms of silicon dioxide. The silicon dioxide layer is created by the thermal oxidation of the silicon surface at 1000-1200° in an oxygen atmosphere. The base of the chip is silicon doped with boron as shown in Figure 5. The silicon nitride is more impervious to leakage current than silicon dioxide in the presence of aqueous ionic solutions (2).

The development of the IGFET represented the merging of two technologies, ion selective electrodes, and solid state integrated circuits. Figure 6 shows the number of papers in Chemical Abstracts by year for IGFETs (Insulated Gate Field

Effect Transistors), ISFETs (Ion Sensitive Field Effect Transistors), and CHEMFETs (Chemically sensitive Field Effect Transistors). ISFETs and CHEMFETs are made with IGFETs. Figure 7 reflects total activity in the area as a percentage of all papers in Chemical Abstracts for each year. The apparent downturn in 1990 of FET activity shown in Figure 6 follows the general downturn in publications for that year. This reflects a softening of research funding during the period. This dissertation shows the feasibility of the IGFET as a microluminometer. Figure 8 shows the growth of research activity in chemiluminescent techniques over the last decade. This figure is the number of papers on chemiluminescent methods in Chemical Abstracts by year. Figure 9 plots the number of luminescent papers divided by the total number of papers each year times 100. This corrects for years with overall less publications, e.g., 1990. Merging IGFETs and chemiluminescent techniques represents the mating of two strong growth technologies.

The author suggests another merging of technologies; that is, IGFET's, silicon micromachining, and recombinant DNA luminescent products to provide the basis for a new generation of 3 dimensional multiresponse biosensors. Silicon micromachining research seeks to make micro 3 dimensional structures. Recombinant DNA techniques are allowing the development of new ways to produce pure luminescent compounds and new luminescent organisms. The author suggests that the IGFET may be modified by silicon micromachining techniques to allow extremely small quantities of new recombinant DNA luminescent products to be immobilized in a three dimensional well. This device will allow both light and ion sensing.

The growth of fiber optic chemical sensors has outpaced the development of optical sensors to complement their implementation in novel applications of analyte

detection. These sensors use fiber optic components with cores usually >10 microns and <150 microns in diameter. The size and configuration of the IGFET makes it an attractive option for optical detection with waveguide chemical sensors (3). These concepts are discussed further in the conclusion of this work.

This dissertation;

1. outlines other workers' studies with the IGFET
2. reviews the operation of the IGFET as an ion sensor
3. offers a brief review of photovoltaic devices
4. describes the instrument constructed by the author for probing the IGFET with photons
5. presents the wavelength response experiments
6. explains the initial experiments
7. demonstrates the IGFET as a detector for recaequorin
8. details the flow injection analysis microluminometer built with the IGFET, and presents and interprets the data collected
9. makes suggestions for future studies.

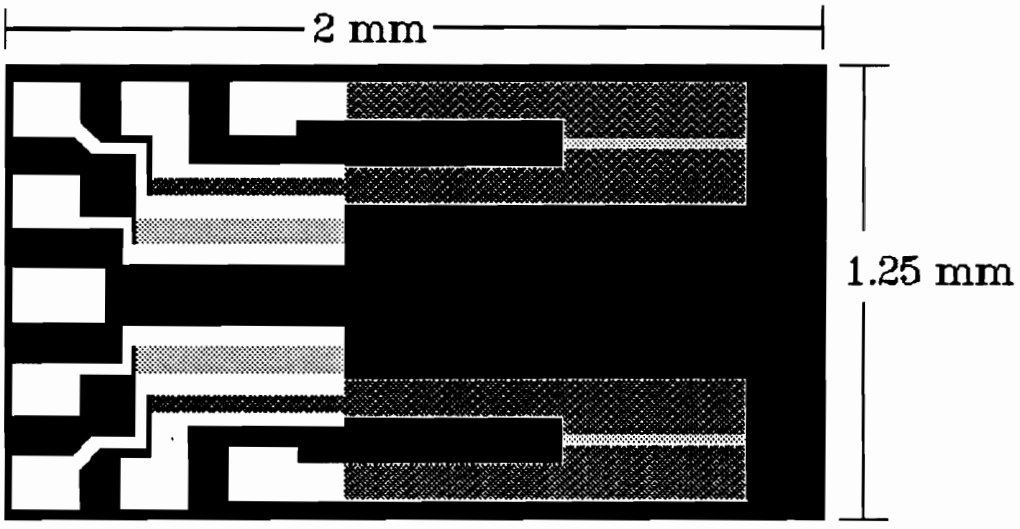

Figure 1 IGFETS chip dimensions

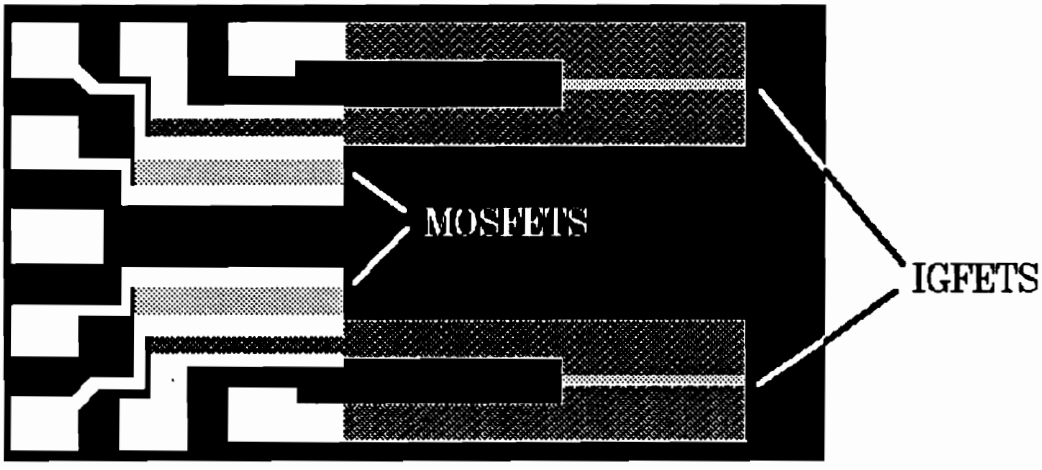

Figure 2 Two MOSFETS and Two IGFETS per chip

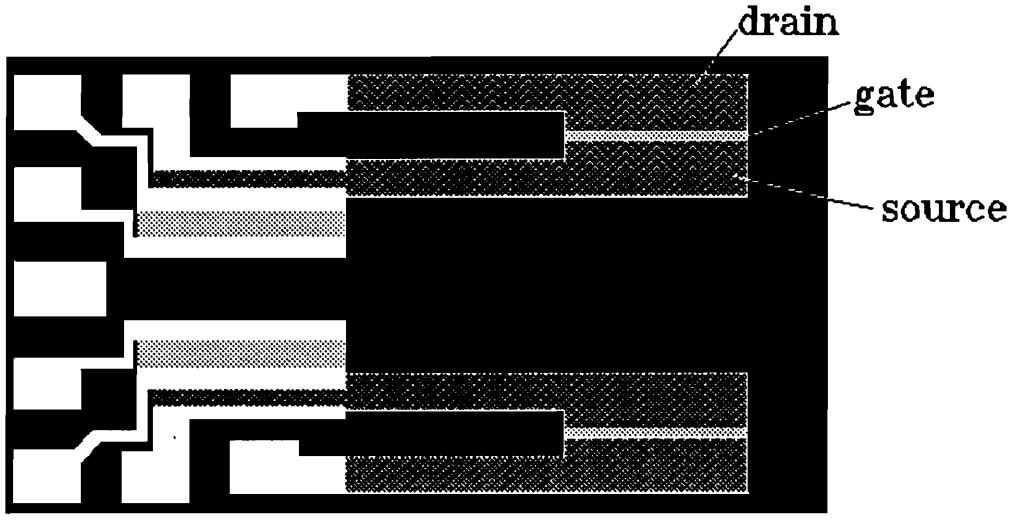

Figure 3 IGFET drain, source, and gate

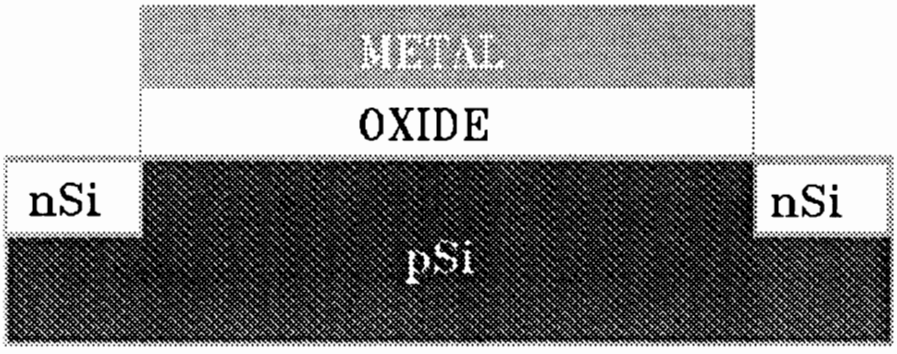

Figure 4 MOSFET side view (not to scale)

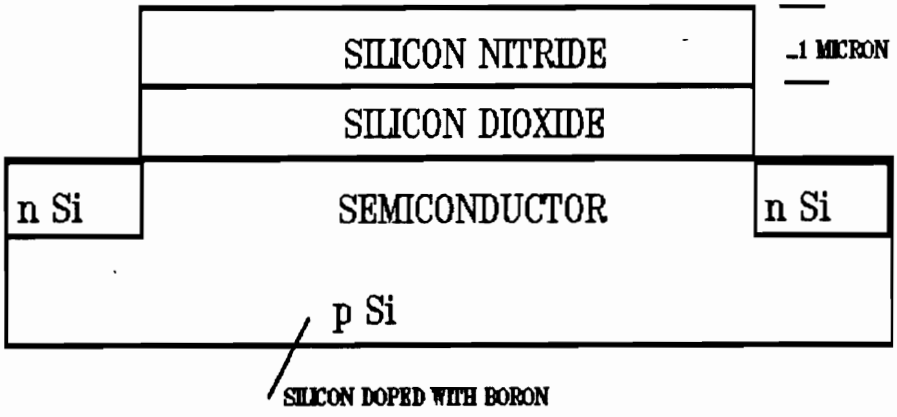

Figure 5 IGFET side view (not to scale)

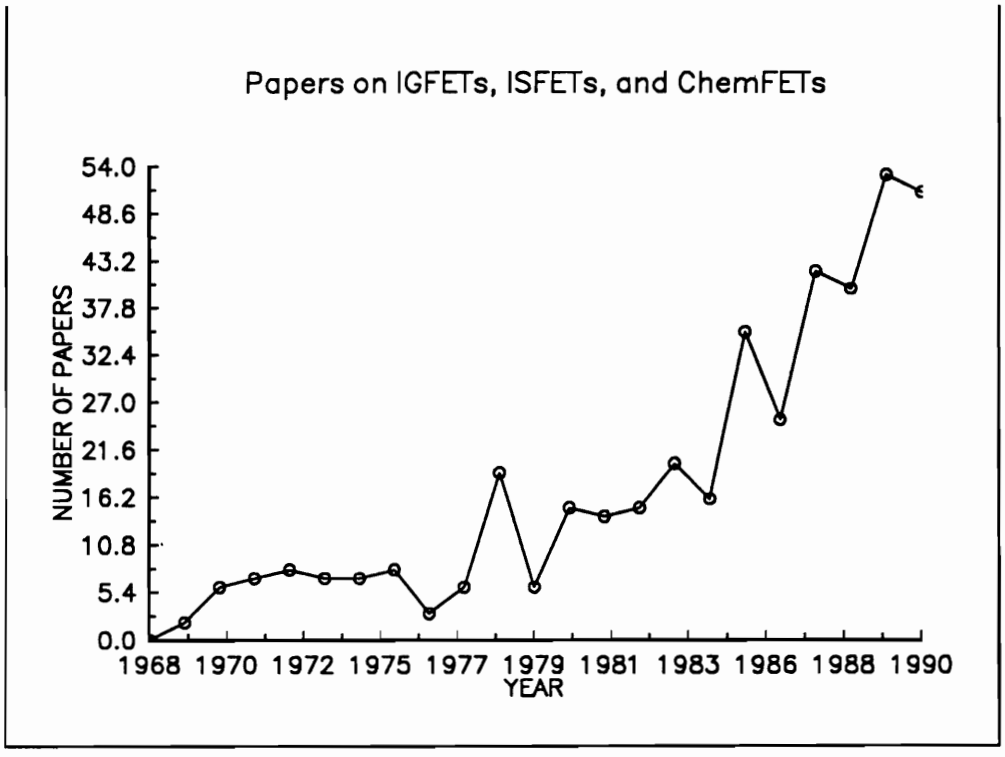

Figure: 6 IGFET, ISFET, and ChemFET papers

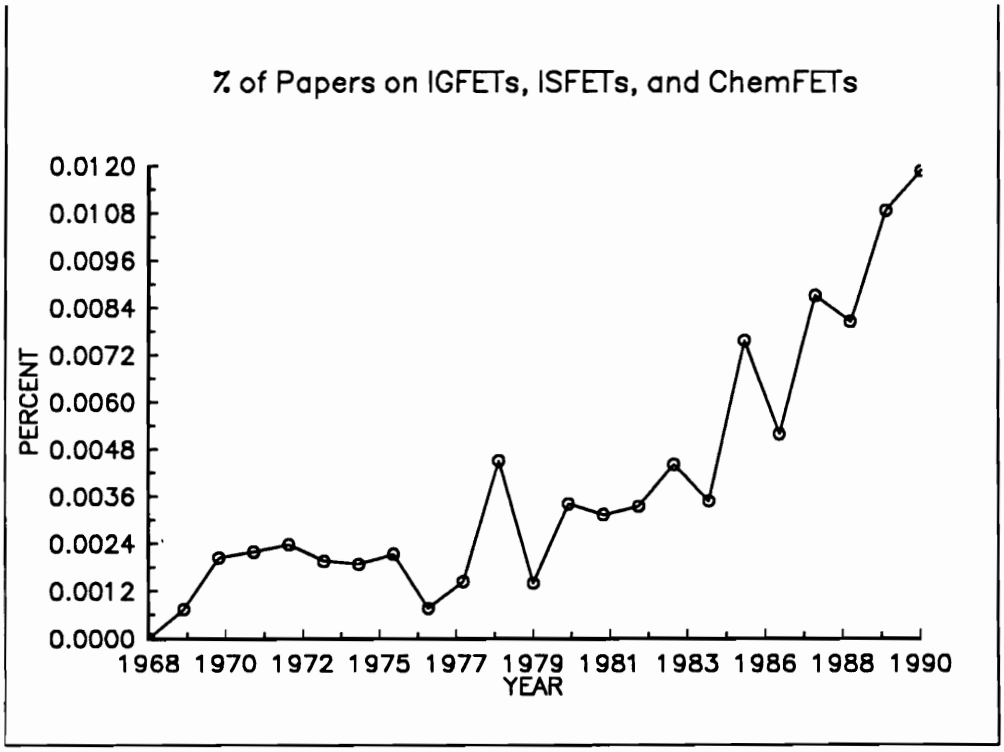

Figure: 7 Percent of total papers per year

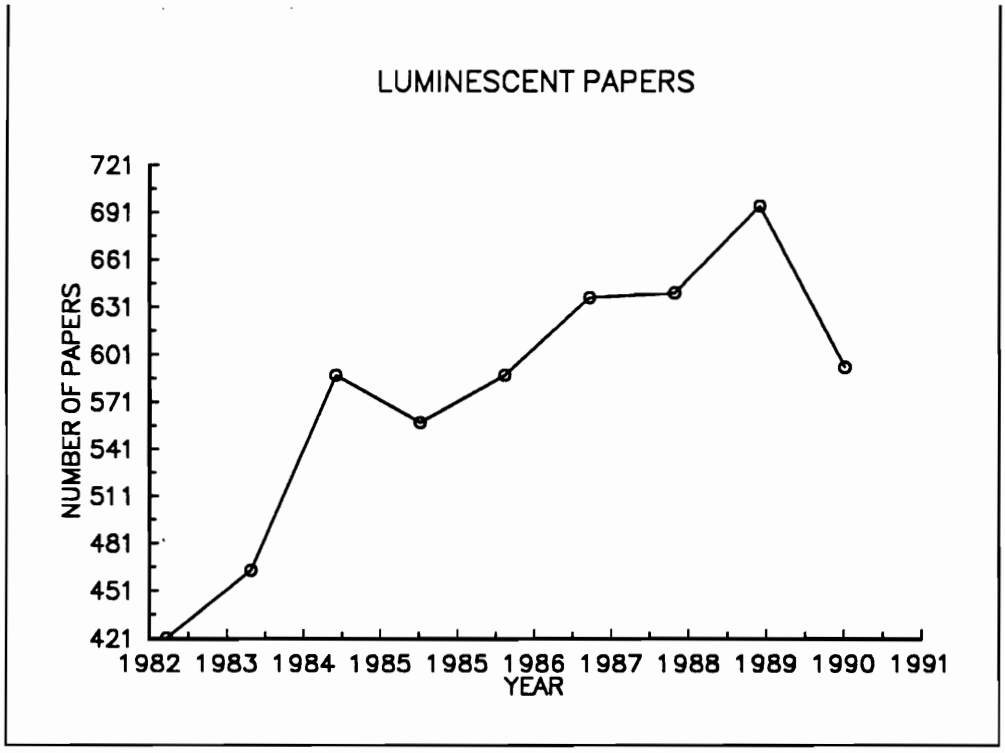

Figure: 8 Luminescent papers per year

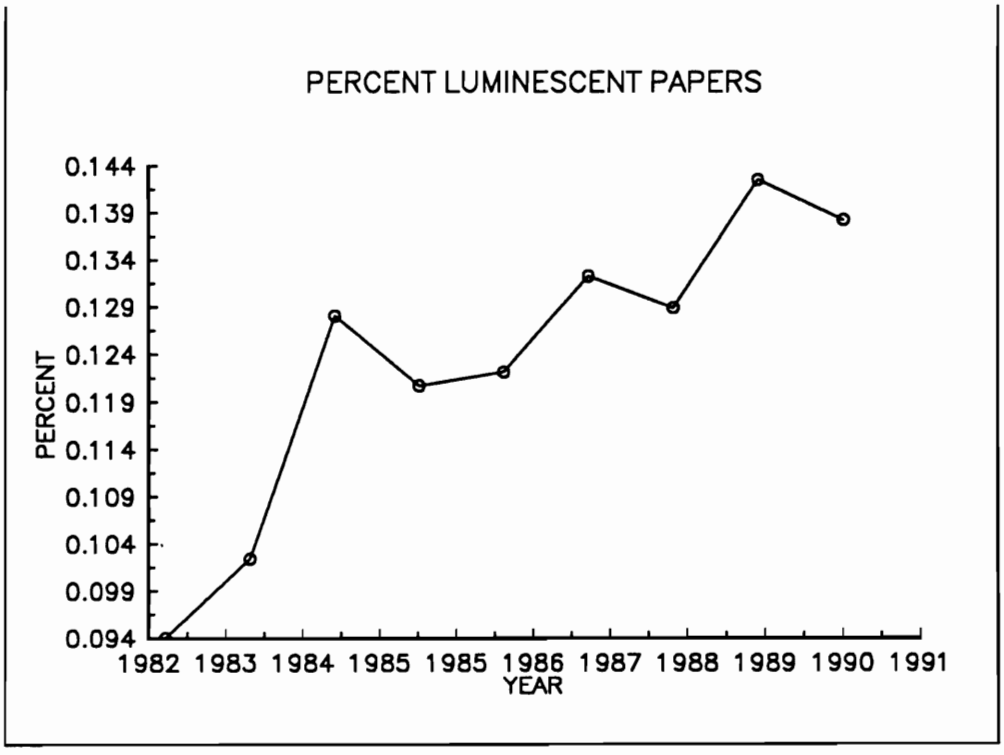

Figure: 9 Percent luminescent papers

2. HISTORICAL

2.1 Introduction

In 1970 Bergveld reported the first development of the insulated gate field effect transistor (IGFET) as an ion sensing device (1). He reported it as an ion-selective device for neurophysiological measurements. Silicon dioxide at the gate imparted sensitivity to hydrogen ions. Since then much work has been done in the development of its uses for the IGFET. Literature references (4, 2, 5, 6) give excellent overviews of the fabrication, theory, and use of the IGFET.

Using an IGFET requires making numerous decisions. This work does not consider the fabrication of IGFET's since the raw material was chips constructed at the University of Utah. Starting with the chip, decisions must be made about how to make electrical connections to the chip, what support to mount the chip upon, how to encapsulate all but the active area to prevent electrical short circuits, how to get analyte to and from the chip, and what type of circuits to use to monitor the signal from the chip.

Research work on IGFET's falls into areas demarcated by the above decisions. Workers are seeking better ways to package the IGFET to improve the ease of handling, increase lifetime, and reduce lateral charge dissipation at the gate area. They also seek novel chemical systems to put on the gate to expand selectivity, new analyte transport systems, and better signal monitoring and conditioning methods.

2.2 Control circuits, Packaging, and Reference Electrodes

Janata and Huber's classic 1979 paper on ion sensitive field effect transistors is a good starting point for a worker new to the subject (7). Bergveld has published circuit principles for parameter control of IGFETs (8). Circuits either hold the reference electrode at a constant potential and measure the change in current through the FET or they measure the change in potential necessary to hold the source/drain current constant. Some recent packaging work includes silicon micromachining (9) techniques to seek better methods for holding membranes at the gate area of the chip. Photocured encapsulation techniques (10, 11) have been developed to circumvent the necessity of tediously applying epoxy. Workers have integrated a differential amplifier into the construction of the chip (12). There is also ongoing work on the design of reference electrodes for the IGFETs (13). The initial systems used standard size reference electrodes which were modified for use with the IGFET. However, the advantage of the small size of the IGFET is largely lost. Workers have sought to miniaturize the reference electrode and to incorporate it in the construction of the device. Comte and Janata built a reference electrode directly on the chip by building a small cavity and filling it with a buffer. The buffer cavity and sample solution were connected by a capillary liquid junction (14). McBride and Janata reported sterilizing a conventional reference microelectrode with ethylene oxide for *in vivo* use with IGFET based ion sensitive electrodes (15).

2.3 Temperature and Time

The effect of temperature on the performance of the IGFET has also been studied (16, 17, 18). The temperature characteristics are a complex function related to the reference electrode, electrolyte, interfacial potential, and device threshold voltage. The response time of IGFET's is of interest. McBride et al. showed that a shorter response time for IGFET based ion sensitive electrodes compared to standard ISE's should not be expected. They found the response time is limited by a diffusion layer at the membrane-solution interface. This outweighs the advantage of not having the parasitic capacitance of the electrical lead between the membrane and the amplifier (19). Comparisons have been made in time response between different IGFET based ion sensors. For example, a Ta pentoxide gate shows a response time of approximately 0.5 ms to pH changes. A pNa-ISFET was much slower responding to [Na+] changes (20), giving a response time of 50ms.

2.4 pH and Ion Sensing with IGFETs

Some of the first work with IGFETs was for pH sensing (21). Silicon nitride is a common gate material used for pH sensing (22). Studies have been done to improve the understanding of the interaction between hydrogen ions and silicon nitride (23). Variations of the gate material have been explored as pH sensing materials (24, 25, 26, 27).

There are some novel uses of the IGFET for pH sensing. Those uses include; a dipstick for titrations (28), a pH-pressure sensor for esophageal studies (29), a microprobe for blood serum pH (30), and an oral pH sensor that transmits the pH in the mouth of the patient to a receiver worn on the belt. (31). Gate materials have been developed for sensing various ions. For example, sodium (32, 33, 34), ammonium (32), chloride (35, 36), potassium (37, 38, 39, 40, 41, 42, 43) and fluoride (44) ions have all been studied.

Van den Vlekkert et al. reported using glass to encapsulate individual sensors and to immobilize hydrogels and membranes. They reported building devices with a pH-sensitive, a potassium-sensitive, and a calcium-sensitive ISFET (45).

Janata et. al. have reported an automated IGFET based system for potentiometric stripping determination of lead (II) and cadmium (II) (46). IGFET systems have been reported for carbon dioxide (47) and nitrates (48).

2.5 Membranes for IGFETs

New methods for placing membranes on the gate area of the IGFET include Langmuir-Blodgett techniques (49, 50), polymer photochemical and thermal curing (51), highly lipid environments (52), Nasicon ($Na_3Zr_2Si_2PO_{12}$) (53), thin silica layer grafting (54), plasma polymer (55), modified PVC matrix (56), CVD alumina films (57), borosilicate glass (58), and thin films of tantalum pentoxide (59). These various techniques either directly give new selectivity to the IGFET or provide new means for immobilizing ionophores at the gate.

A novel flow-through gate design has been reported (60). This design utilized micro-etching techniques and yielded a three dimensional gate with

increased surface area. Alegret et al. reported using a flow-through IGFET design for constructing a pH-ISFET as a detector in the determination of ammonia in a flow injection analysis system. Ammonium ion was converted to ammonia, which diffused through a microporous hydrophobic membrane into an ammonium chloride recipient stream forming a pH buffer which was monitored by the IGFET detector (61, 62).

IGFET Biosensors

Probably the most active area of IGFET research is the development of IGFET based biosensors. One of the first biosensor applications of the IGFET was the work done by Janata and Caras on a penicillin sensor (63). Penicillinase was immobilized at the gate. Penicillinase catalyzes a ring opening reaction in penicillin which releases hydrogen ions. The hydrogen ions diffuse to the gate of the IGFET and the IGFET measures the localized pH change.

IGFET based biosensors have been reported for glucose (64, 65, 66, 67, 68). Hanazato et. al. photolithographically patterned a glucose oxidase membrane on the gate surface (69). Kimura et. al. put an albumin-based, spin-coated, immobilized enzyme membrane on an IGFET glucose sensor and evaluated it by experimentation and computer simulation (70). His group has also used an IGFET sensor to monitor blood glucose (71, 72).

Urea sensors have been reported by Vlasov (73) and Anzai (74). Chandler et al. reported a IGFET based flow injection analysis determination of urea (75). Sakai has used a urea IGFET based sensor to determine copper (2+) ions (76).

Sensors for nicotinamide (77), acetylcholine(78), and ClO_4^- (79) have been developed. Iida et. al. reported a sensor for monitoring glutamic-pyruvic transaminase activity (80).

Thin membrane techniques for IGFET based biosensors have been developed by Gotoh (81) and Anzai (82). Shoji et. al. reported a IGFET based miniature blood gas analyzer (83) and Takasu (84) implanted IGFET based sensors into the brain and cerebrospinal fluid of a dog to monitor pH changes after total cerebral circulation stoppage. An alcohol sensor was developed by Kitagawa et. al. using immobilized bacteria (85).

IGFET researchers have demonstrated immunosensors for human IgG (86), human serum albumin (87), and theophylline (88). Schasfoort et. al. reported using a IGFET to monitor the potential of a membrane as an immunological reaction took place within the membrane (89). Schasfoort et al. also reported the requirements for the construction of an immunological field-effect transistor (ImmunoFET) that operates on the direct potentiometric sensing of protein charges (90). Selectivity of the ImmunoFET was obtained by immobilizing antibodies on the gate area of the ISFET, enhancing the surface affinity to the corresponding antigens over other molecules in the solution. A theoretical approach has been developed to provide an insight into the potential and ion distribution in the protein layer on the ImmunoFET.

The use of the IGFET as an optical sensor is obviously a new application area for the device.

3. THEORETICAL

3.1 The IGFET as an ion sensor

The insulated gate field effect transistor is a descendant of a semiconductor device called a MOSFET, or metal oxide semiconductor field effect transistor. A brief review of semiconductor material will help build an explanation of the MOSFET. A material that is a semiconductor has an electrical resistivity between a conductor and an insulator. Resistivity is a measure of how well the substance inhibits the flow of electric current in the presence of an electric field.
A silicon based semiconductor is made by introducing some other atoms, e.g., phosphorus or boron, into the silicon lattice. When phosphorus, with five valance electrons, is used, there is one extra electron beyond what is needed for sigma bonding. This extra electron is called a conduction electron. Semiconductors with conduction electrons are called n-type. If boron is used there is one less electron than necessary to complete the sigma bonds. This vacancy is called a hole. Semiconductors with holes are called p-type. Actually, both types of semiconductors have both conduction electrons and holes, but the n-type has an excess of conduction electrons and the p-type has an excess of holes. N-type silicon next to p-type silicon is called a pn junction. This is a diode.

Consider the circuit shown in Figure 10. Note that the n-type silicon (n-Si) is biased negative relative to the p-type silicon (p-Si).

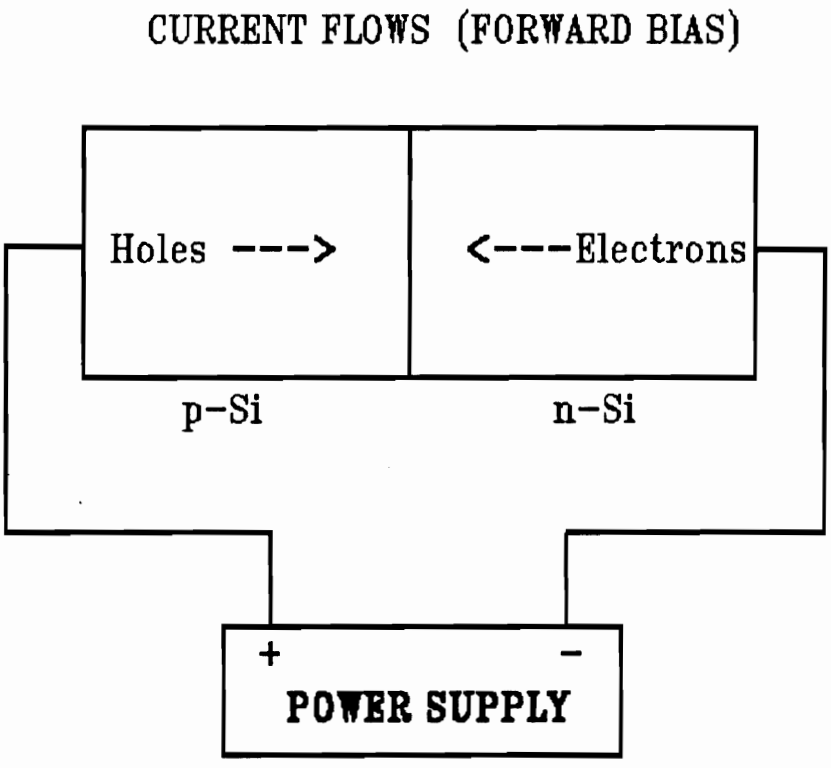

Figure 10 Forward Biased pn Junction

Electrons flow from the power supply into the n-silicon. At the junction the electrons and holes combine. When the electrons leave the p-silicon and return to the power supply then new holes are created in the p-silicon. A pn junction wired with this polarity is forward biased. A silicon pn junction must have a forward bias of at least 0.6 volts for a current to flow.

In Figure 11 the polarity of the pn junction is reversed. Since the electrons and holes are moving away from the junction, an approximately one micron wide area devoid of conduction electrons and holes is formed. This is called the depletion region. In this circuit the diode is reversed biased and no current flows unless the voltage gets high enough to cause a breakdown to occur.

In the introduction, the geography of the MOSFET was presented. Figure 12 again shows a side view not-to-scale of the MOSFET. The base of the chip is constructed of p-silicon. The areas of n-silicon in the top right and left corners of the chip are the source and the drain. The gate area above the base is covered by a layer of silicon dioxide. There is a layer of metal above the silicon dioxide layer.

In Figure 13 the source is connected to the negative side of a power supply and the drain is connected to the positive side. Note that the base drain interface is a reversed biased pn junction. Therefore a depletion layer occurs as indicated in Figure 13 and no current flows.

In Figure 14 the positive side of another power supply is connected to the gate metal. The positive charge at the gate attracts electrons to the top of the base. A thin channel of electrons forms and current can flow between the source and drain.

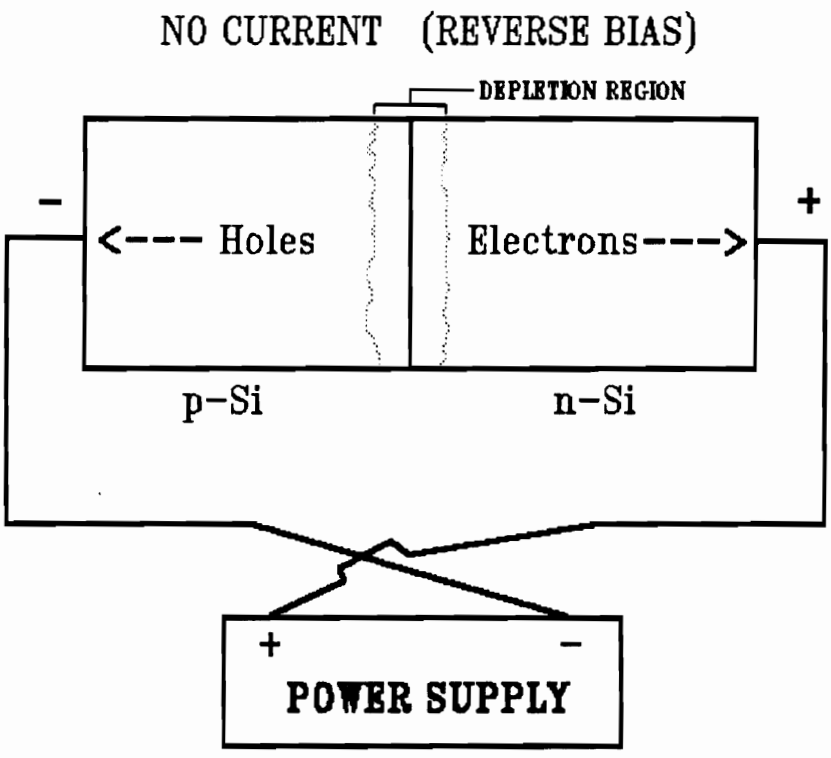

Figure 11 Reverse Biased pn Junction

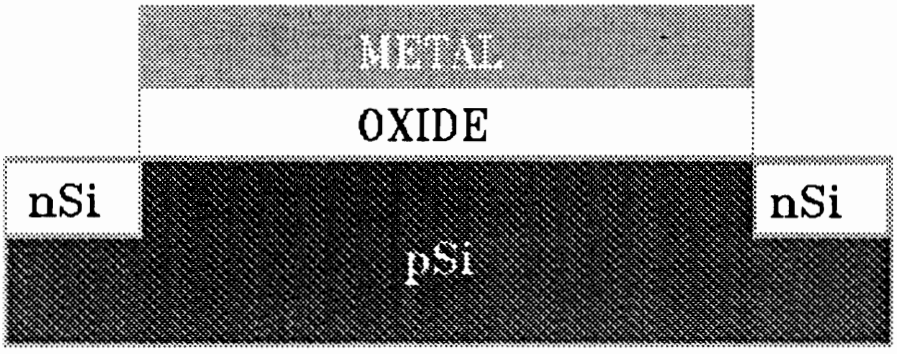

Figure 12 A MOSFET side view (not to scale)

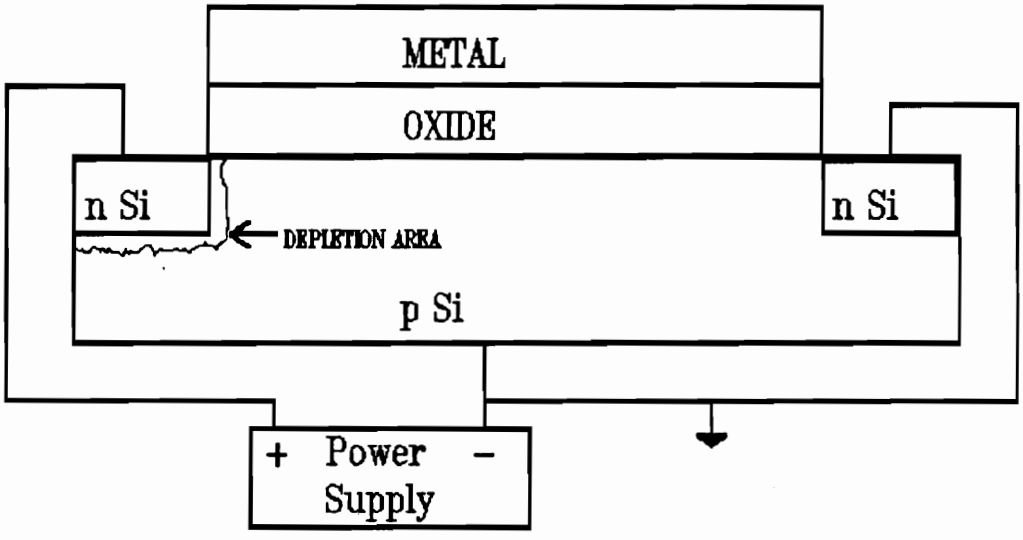

Figure 13 MOSFET with power supply

Note the silicon dioxide, an insulator, prevents current from flowing between the gate and the base. If the positive gate voltage is increased then the current between the source and drain increases. Therefore, the gate potential (charge on the gate) controls the current that flows from source to drain. In the term - field effect transistor - the field effect refers to the charge on the gate. The gate potential which must be applied to create a strong inversion is the threshold voltage, V_T, given by

$$V_T = - Q_B/C_0 + 2\phi_{FERMI} \qquad 1$$

where Q_B is the charge per unit area in the surface space-charge and C_0 is the capacitance per unit area of the insulator. The first term on the right side of the equation represents the portion of the applied voltage which is dropped across the insulator while the second term represents the portion of the applied voltage which is dropped in the surface of the silicon. Equation 1 applies only to an ideal metal oxide semiconductor. Three terms are added to the ideal case to account for non-idealities which are grouped into a single term called the flat-band voltage, V_{FB} where

$$V_{FB} = \Phi_{MS} - Q_{SS}/C_0 - 1/C_0 \int_0^d x/d\ r(x)dx. \qquad 2$$

Φ_{MS} is the work function difference between the metal and the semiconductor. The other two terms are for surface charge and dispersed charge in the insulator layer respectively, where x is the distance from the metal-insulator interface, r(x) is the charge density as a function of x, and d is the thickness of the insulator. Equation 1 and 2 combine to give

$$V_T = V_{FB} - Q_B/C_0 + 2\phi_{FERMI}. \qquad 3$$

Figure 15 shows that for a model of the field effect transistor, vertical charge is related to horizontal current. The charge build up on either side of the silicon dioxide, a dielectric, is equivalent to what occurs in a capacitor. This is shown in Figure 16. It is important that this charge buildup not be lost to current flow through the dielectric or dissipation across the surface of the chip. The drain current, I_D, is expressed

for $V_D < V_{Dsat}$ by

$$I_D = \mu_n WC_0/L(V_G - V_T - V_D/2)V_D \qquad 4$$

for $V_D > V_{Dsat}$ by

$$I_D = \mu_n WC_0/L(V_G - V_T)^2, \qquad 5$$

where μ_n is electron mobility in the channel, W is the width of the gate, C_0 is the capacitance of the insulator, L is the length of the channel, V_G is the applied gate voltage, V_T is the threshold voltage, V_D is the drain voltage, and $V_{Dsat} = V_G - V_T$.

Figure 17 is a diagram of an IGFET. Note that it is constructed the same as the MOSFET, except there is no metal layer above the oxide layer at the gate. Figure 18 shows the conditions necessary to make the IGFET into a chemical sensor. The solution of interest must come in contact only with the gate area. The remainder of the surface of the chip must be protected or short circuits will occur. Hydrophobic epoxy is used to cover the areas that require protection from the solution. Note that the oxide layer consists of two layers. There is a layer of silicon nitride above the silicon dioxide layer. The silicon nitride allows less leakage current than silicon dioxide in the presence of an aqueous solution, since the silicon dioxide hydrates more readily than silicon nitride.

With the silicon nitride exposed to the solution the chip will function as a pH sensor. An ion exchange reaction occurs between the hydrogen ions and the silicon nitride surface. Other materials are placed on the silicon nitride to make a sensor selective for species other than hydrogen ions. The basic mechanism of operation is the same for the IGFET as for the MOSFET. Charge at the gate controls the current flowing from source to drain. If a variation in concentration of the species of interest is related to a change in charge at the gate then the concentration of the species can be related to the current flowing from source to drain. Another difference from the MOSFET is the use of a reference electrode in the solution. The reference electrode is connected to the source and base. The equations for the drain current, I_D, for the IGFET in solution are expressed

for $V_D < V_{Dsat}$ by

$$I_D = \mu_n W C_0/L(V_G - V_T^* - E_{ref} - \phi_{sol\text{-}mem} - V_D/2)V_D, \text{ and} \qquad 6$$

for $V_D > V_{Dsat}$ by

$$I_D = \mu_n W C_0/2L(V_G - V_T^* - E_{ref} - \Phi_{sol\text{-}mem})^2 \qquad 7$$

where V_G is the voltage applied to the reference electrode, E_{ref} is the potential at the reference electrode-solution interface, $\phi_{sol\text{-}mem}$ is the potential at the solution-membrane interface, and

$$V_T^* = V_T - \Phi_{m\text{-}sol} - \Phi_{sol\text{-}mem} = \Phi_{mem\text{-}s} - Q_{ss}/C_0 - Q_B/C_0 + 2\phi_F \qquad 8$$

where $\Phi_{m\text{-}sol}$, $\Phi_{sol\text{-}mem}$, and $\Phi_{mem\text{-}s}$ are the work function differences between the metal and solution, solution and membrane, and membrane and semiconductor, respectively (2).

The IGFET can be operated so the potential of the reference electrode is held constant and the current from source to drain is measured. Alternatively, the potential necessary to hold the current constant can be the signal that is measured.

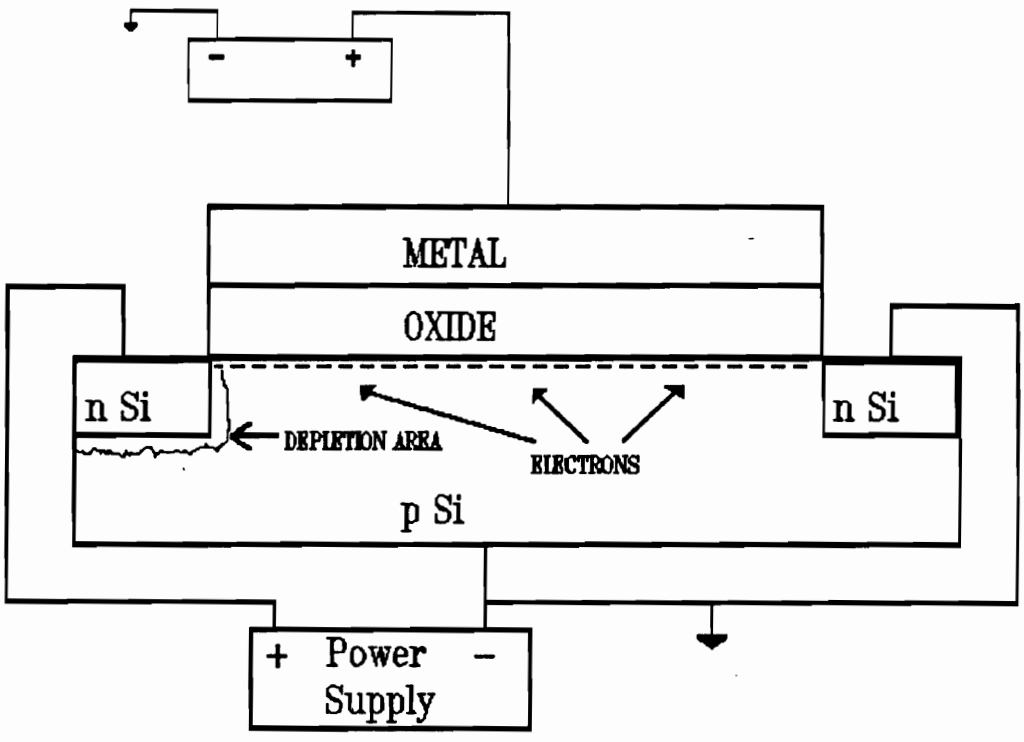

Figure 14 Formation of an inversion layer

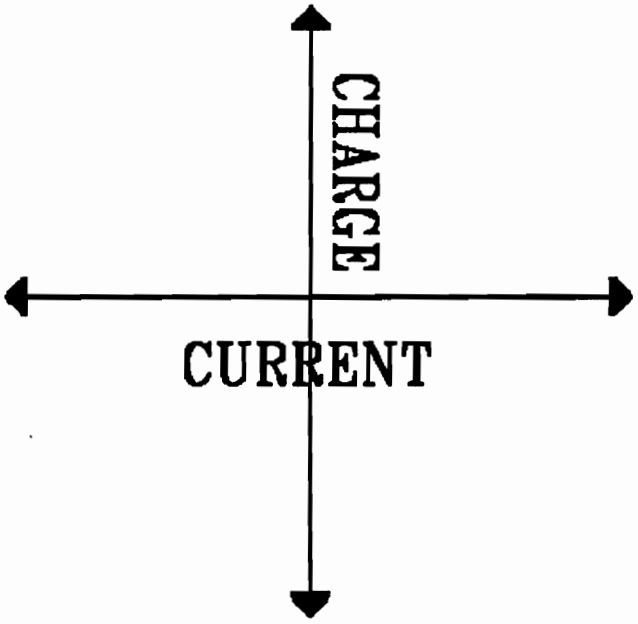

Figure 15 2 Dimensional model

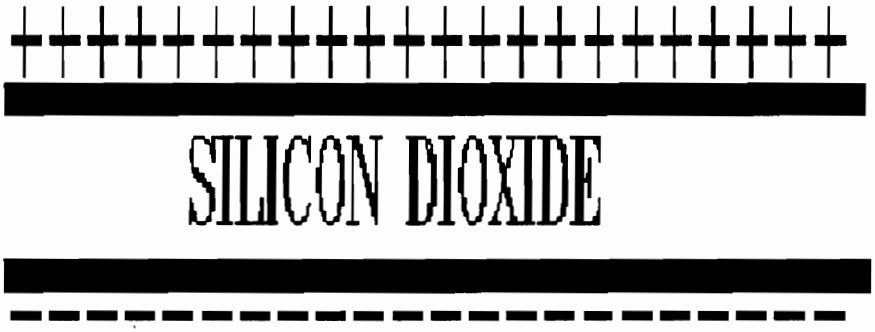

Figure 16 Charge buildup viewed as a capacitor

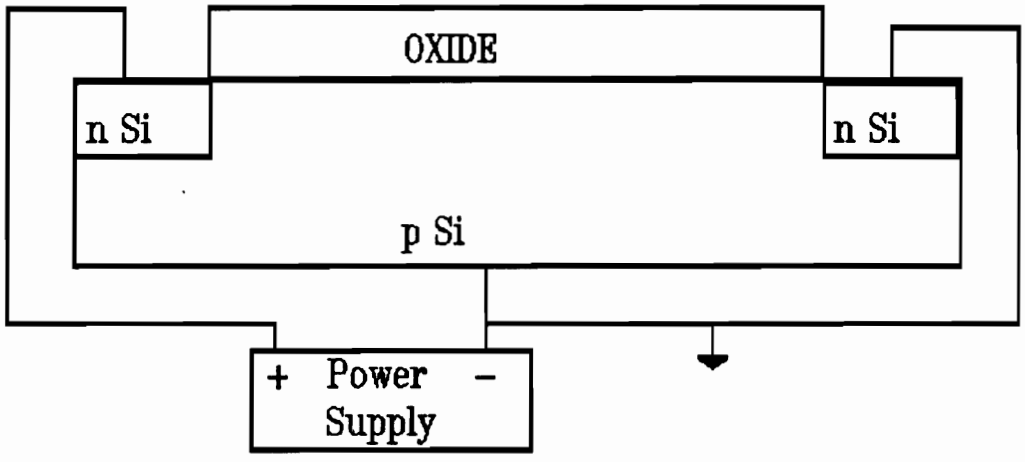

Figure 17 IGFET

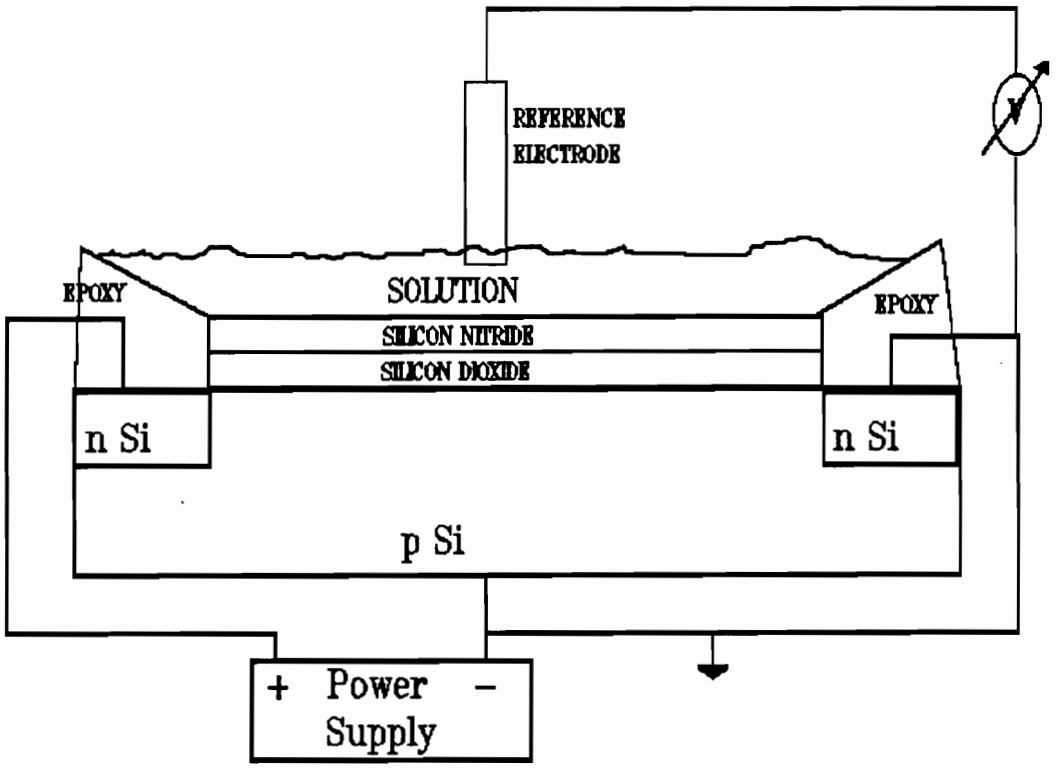

Figure 18 IGFET as a chemical sensor

3.2 The IGFET as an optical sensor

In considering the IGFET as an optical sensor one of the first questions is whether the traditional field effect operation of the device is involved in its operation as an optical device. This question is addressed in the experimental section.

The mechanism for converting optical energy into some form of electrical energy, i.e., current, voltage, conductivity, capacitance, or resistance, is named the photovoltaic effect. The inverse mechanism, converting electrical energy into optical energy, is called the electroluminescent effect. Thermal detectors and quantum detectors are two broad classes of optical detectors.

Thermal detectors respond to the change in temperature after radiation is absorbed and transformed into heat. The heat generated within the device may alter a junction potential, e.g., a thermocouple, or the heat may cause a change in the resistance of a material, e.g., the thermistor bolometer. Thermal detectors do not directly convert the absorption of photons into charge carriers, but the electrical effects are secondary effects that result from the change in temperature. Thermal detectors are not selective with respect to wavelength. Thermal detectors are used mainly in the infrared region.

Quantum detectors respond directly to the incident photons. The absorbed photons interact directly with the atoms and molecules of the detector. Quantum detectors' response varies with the wavelength of the incident photons. Quantum detectors have a faster response and higher sensitivity than thermal detectors. Quantum detectors are used mainly in the UV-visible region.

Quantum optical detectors fall into two groups called photoconductive detectors and photovoltaic detectors. The photovoltaic detector is the only quantum detector not requiring a bias voltage supply. Since the IGFET can operate as an optical detector without a bias voltage supply, then the IGFET is classified as a photovoltaic quantum optical detector.

Some confusion is caused by the photoconductive vs. photovoltaic classification nomenclature since photovoltaic detectors can be operated in a photoconductive mode. Therefore, another method of classification is often used. This method is based on the presence or absence of a junction in the semiconductor material. This method classifies detectors composed of homogeneous uniform semiconductor material as bulk detectors. Detectors that have a pn junction or some modification of a pn junction are classified as junction semiconductor detectors. The IGFET is a junction semiconductor optical detector based on this classification scheme since the IGFET contains pn junctions.

Figure 19 shows the energy relationship of the valence band and the conduction band. An electron-hole pair is generated when the electron gains sufficient energy from photon absorption to be promoted from the valence band level to the conduction band level. Recombination occurs when the electron returns to the energy level of the valence band. The energy level between the highest valence band energy, E_V, and the lowest conduction band level, E_C, is called the forbidden gap, described by the term, E_g. Current from the photovoltaic detector is the result of photons incident on the pn junction producing additional electron-hole pairs (91, 92).

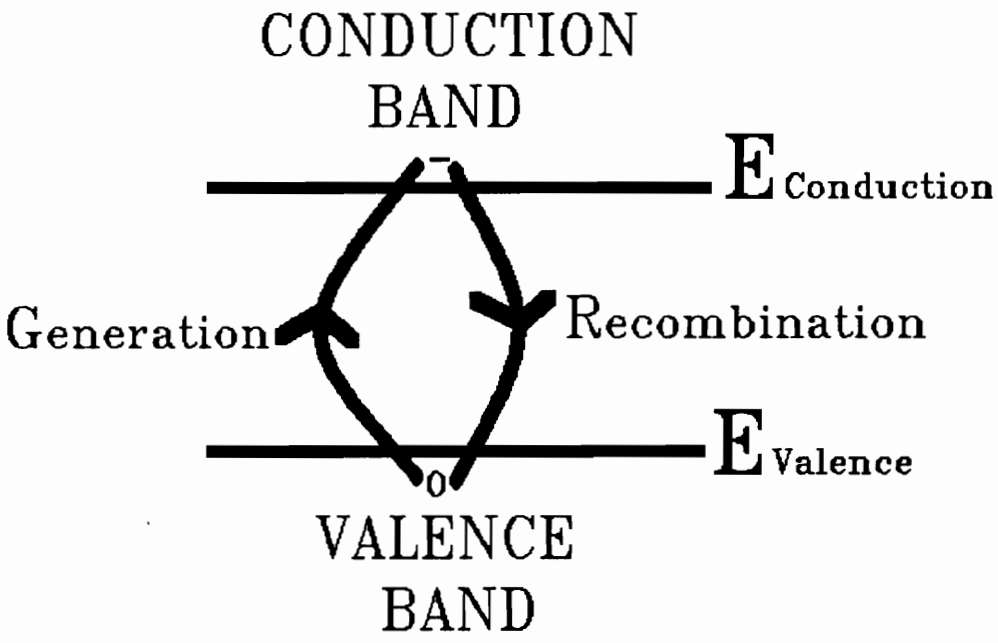

Figure 19 Energy diagram

4. IGFET LIGHT SENSING CHARACTERISTICS

4.1 Surface study

One of the first steps in evaluating the IGFET as an optical sensor was to perform a surface study to ensure that there were no unexpected coatings present on the chip. There was concern that a coating may have been used in the production of the IGFET which does not involve its operation as an ion sensor but would effect its characteristics as an optical sensor.

Auger electron spectroscopy (AES) was chosen to probe the IGFET surface. Auger electron spectroscopy uses an incident high-energy electron (2-3 keV) to eject an inner electron from a surface atom. An electron further out in the atom falls into the vacancy and the released energy is given to an outer electron which is the ejected electron detected by the Auger instrument. The ejected electron is called an Auger electron. The kinetic energy of the Auger electron is related to the energy of the electron that filled the vacancy. The Auger spectrum is mainly the series $(E_k - E_{L1}) - E_i$, where the *i*th type of outer electron is ejected (93).

It is possible to focus the incident electron beam to a diameter useful for probing the IGFET's surface. A 5 micron diameter 3keV beam was used. Analysis was performed on the area of the chip indicated in Figure 20. This area was picked to include some of the gate, drain, and field nitride areas of the chip. Nothing unexpected was found. There were strong peaks for silicon and nitrogen (Figure 21). No evidence of any other element except a small amount of oxygen was detected. This is presumably due to surface adsorption.

Figure 20 Area of IGFET for surface study

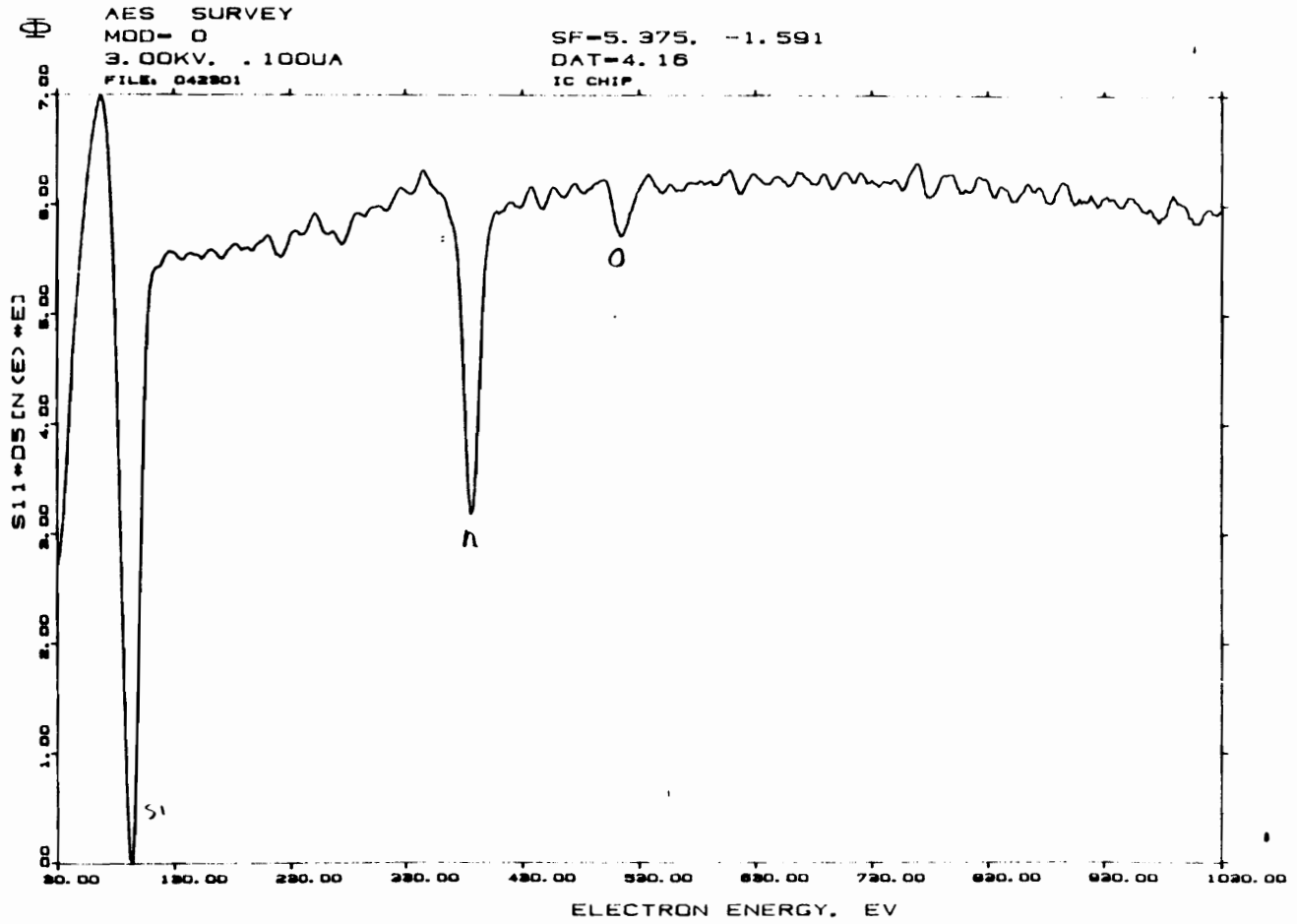

Figure 21 Auger spectrum for the IGFET surface

4.2 Photon probe

The instrument shown in Figure 22 was designed and built to determine which part of the IGFET is light sensitive. An optical fiber with a 4 micron diameter core was used to give a light pattern much smaller than the surface area of the IGFET (1.25 x 2 mm). The IGFET assembly was mounted on a translational stage which moved the chip across the path of the light emitted from the fiber. The knob on the translation stage was marked with twenty-five increments, each representing 20 microns of stage movement. The chip's output vs. location of light was recorded.

A 26.1 x 7.5 x 5 cm aluminum block with milled surfaces provided the foundation for the instrument. A Tekna Micro-Lite flashlight served as the light source. The flashlight was modified to operate from an external 3 volt supply to give a more stable source intensity. The flashlight was held in a brass ring by a set screw and the ring was mounted to a base via an aluminum post. The flashlight was fitted to the rear of a ten power microscope objective (Swift #820493) which was held in a similar rig as the flashlight.

The light from the microscope objective was launched into the 4 micron core optical fiber (94). The optical fiber (Newport Corporation F-SV, 4 micron core, 125 micro cladding, and 200 micron jacket) was stripped of approximately one centimeter of its jacket at each end of the fiber. A fresh razer blade was used to strip the jacket (95). A scribe was used to cleave the fiber.

The fiber was held by a brass chuck in a translational stage. The stage was connected to the foundation via an aluminum post and base. More information on handling small core fibers may also be obtained from reference (96).

The IGFET was glued to a substrate and wirebonds connected between the chip and nine of the substrate's sixteen legs. Figure 23 is a photograph of the chip glued to the substrate. The substrate was connected to a translation stage via a Plexiglass cylinder (0.3cm dia. x 2.3cm long) and a piece of aluminum (1.2 x 1.2 x 4.6 cm). The Plexiglass cylinder end surface was machined in a lathe to provide a flat surface perpendicular to the length of the cylinder. The substrate was glued to this surface. The cylinder was glued in a 0.3 cm. diameter hole drilled through the width (1.2cm) of the aluminum as seen in Figures 24 and 25.

The unused legs of the substrate were amputated at their base and the remaining nine legs were connected to a manifold of connectors via wirewrap connections. Two wires were soldered to the center post and ground of a cable connector in an aluminum strain relief bar. Pins, which fitted the manifold sockets, were wirewrapped to the other end of the two wires. This arrangement allowed connection between the cable and any two of the nine chip connections as seen in Figure 25.

The cable was connected to a Keithley 414 microammeter. The ammeter was set to one nanoamp full scale. The data were collected with a digital voltmeter at the voltage output of the microammeter.

The fiber was positioned near the surface of the chip. A forty power field microscope was then used to view the fiber and chip while adjusting their relative position to within a few microns of each other. The high reflectivity of the IGFET chip surface made this difficult since both the fiber and the fibers reflection are seen through the microscope. Figure 26 shows where the fiber was positioned. The dotted line in the figure shows the path the fiber followed when the translation stage knob was turned and the chip is moved.

The experimental data represents four runs. One run for the source and drain of each of the two IGFET's on the chip. The chip was moved to the zero position as noted above. Connection was made to the component of interest, e.g., the first drain. The voltage at this point was recorded and the stage was moved one unit and the new voltage was recorded. This process was continued until the area of interest was scanned and the voltages return to baseline values. The numbering of the source and drains in shown in Figure 27. The results for the four runs are shown listed in Table 1 and plotted in Figures 28 and 29.

The results show the source and drain areas of the chip are light sensitive and the gate areas are not. Figure 29 shows the data superimposed on a diagram of the chip with each insulated gate represented as a vertical black bar. The gate areas fall between the peaks. If only the gate areas are light sensitive then there would be two peaks, i.e., one over each gate area. The area between 0 volts and the baseline represents the chip response to the ambient light in the near-dark room.

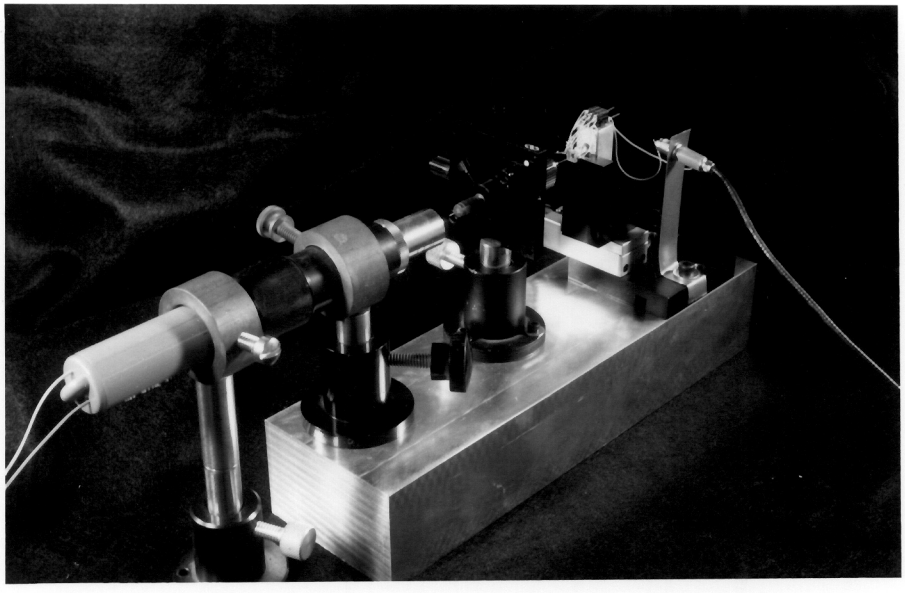

Figure 22 Photograph of the Instrument

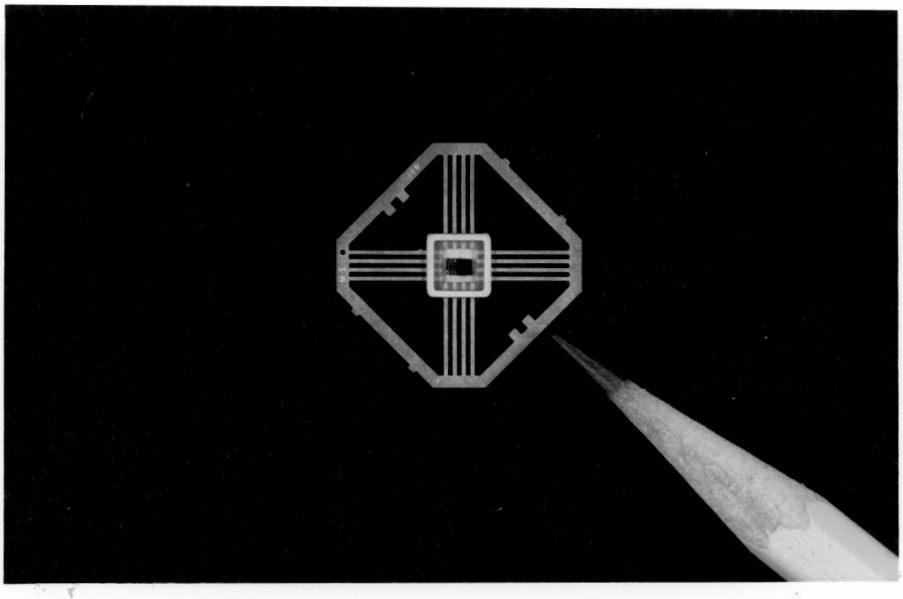

Figure 23 photograph of the chip on substrate

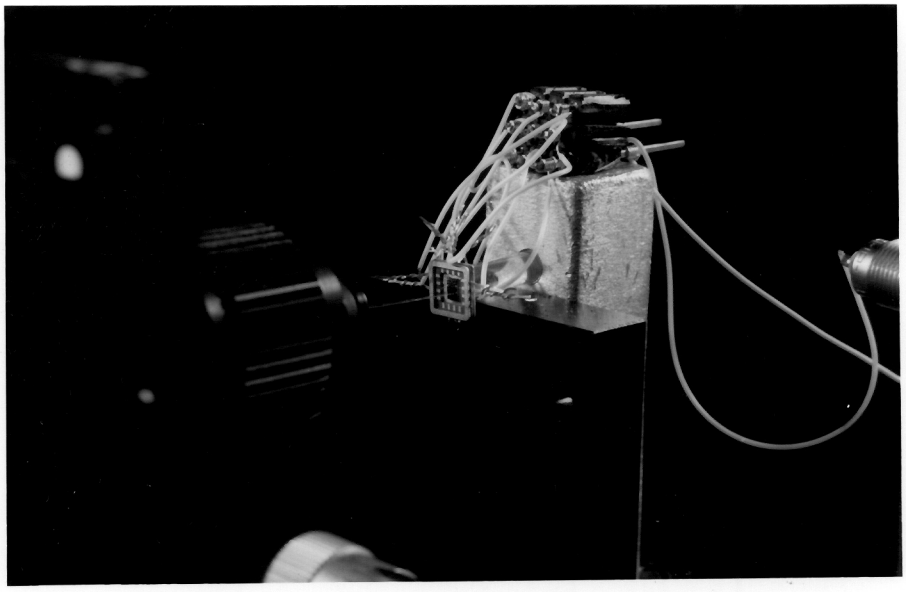

Figure 24 Photograph of the optical fiber at the chip surface

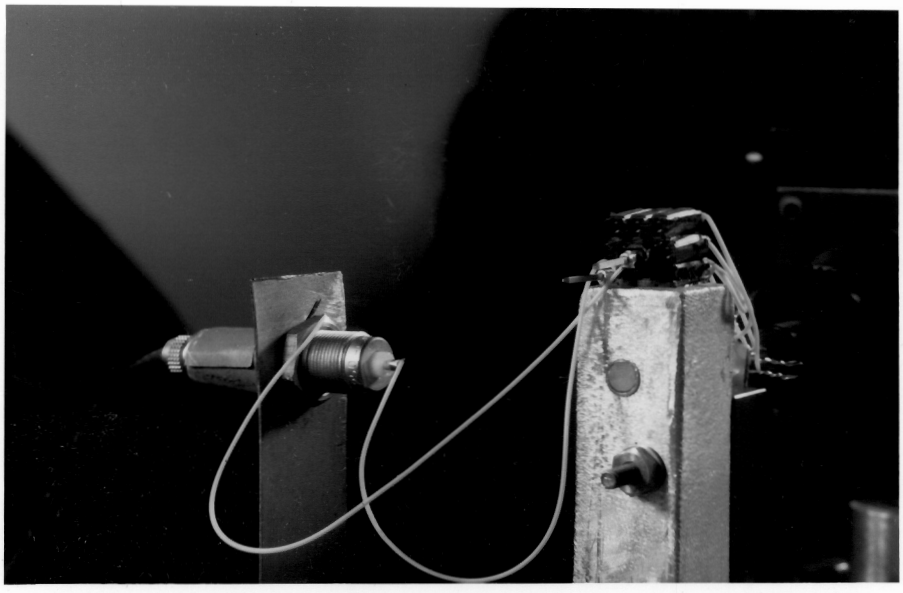

Figure 25 photograph substrate, cylinder, and aluminum

Table 1 Data for the photon probe experiment

POSITION	1	2	3	4
0	0.48	0.56	0.4	0.22
1	0.48	0.53	0.4	0.22
2	0.5	0.53	0.4	0.22
3	0.57	0.53	0.4	0.22
4	0.63	0.53	0.4	0.22
5	0.76	0.53	0.4	0.22
6	0.96	0.53	0.4	0.22
7	1.52	0.53	0.4	0.22
8	2.07	0.53	0.4	0.22
9	3.37	0.53	0.4	0.22
10	4.4	0.63	0.4	0.22
11	4.82	0.63	0.4	0.22
12	4.96	0.63	0.4	0.22
13	5.05	0.63	0.4	0.22
14	4.92	0.63	0.4	0.22
15	4.28	0.85	0.4	0.22
16	3.3	0.96	0.4	0.22
17	2.48	1.05	0.4	0.22
18	1.75	1.23	0.4	0.22
19	1.35	1.46	0.4	0.22
20	1.02	1.8	0.4	0.33
21	0.79	2.53	0.4	0.33
22	0.69	3.25	0.4	0.33
23	0.63	4.39	0.4	0.33
24	0.54	5.19	0.45	0.33
25	0.5	5.33	0.45	0.33
26	0.51	4.9	0.45	0.33
27	0.45	4.77	0.45	0.33
28	0.45	4.06	0.45	0.33
29	0.42	2.91	0.45	0.33
30	0.4	2.23	0.45	0.33
31	0.41	1.61	0.45	0.33
32	0.39	1.32	0.45	0.33
33	0.39	1.03	0.45	0.33
34	0.38	0.92	0.45	0.33
35	0.38	0.8	0.53	0.38
36	0.36	0.7	0.53	0.38
37	0.36	0.7	0.53	0.38
38	0.36	0.7	0.53	0.38
39	0.36	0.7	0.53	0.38
40	0.36	0.57	0.84	0.42

Table 1 (cont.) Data for the photon probe experiment

POSITION	1	2	3	4
41	0.36	0.57	0.97	0.42
42	0.36	0.57	1.11	0.42
43	0.36	0.57	1.32	0.42
44	0.36	0.57	1.7	0.47
45	0.36	0.57	2.27	0.47
46	0.36	0.57	3.55	0.47
47	0.36	0.57	4.45	0.47
48	0.36	0.57	4.95	0.47
49	0.36	0.57	5.17	0.66
50	0.36	0.57	5.25	0.83
51	0.36	0.57	5.26	0.88
52	0.36	0.57	5.19	0.98
53	0.36	0.57	4.89	1.18
54	0.36	0.57	4.35	1.5
55	0.36	0.57	3.76	2.12
56	0.36	0.57	3.16	2.73
57	0.36	0.57	2.48	3.52
58	0.36	0.57	1.75	4.47
59	0.36	0.57	1.38	4.9
60	0.36	0.57	1.12	5.15
61	0.36	0.57	1.6	5.16
62	0.36	0.57	0.92	4.99
63	0.36	0.57	0.86	4.24
64	0.36	0.57	0.86	2.95
65	0.36	0.57	0.72	2.1
66	0.36	0.57	0.72	1.28
67	0.36	0.57	0.72	0.95
68	0.36	0.57	0.72	0.81
69	0.36	0.57	0.72	0.73
70	0.36	0.57	0.53	0.68
71	0.36	0.57	0.53	0.68
72	0.36	0.57	0.53	0.6
73	0.36	0.57	0.53	0.57

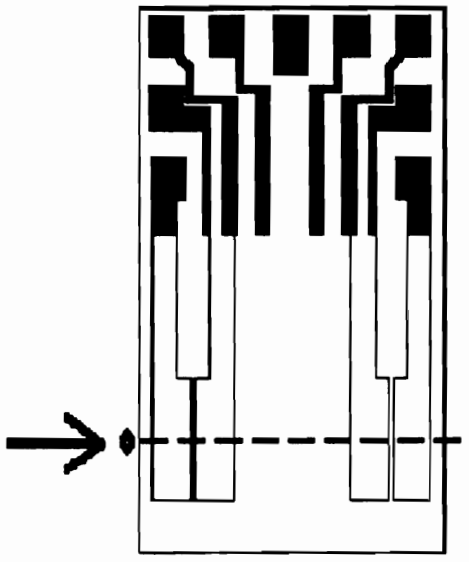

Figure 26 Chip fiber light path

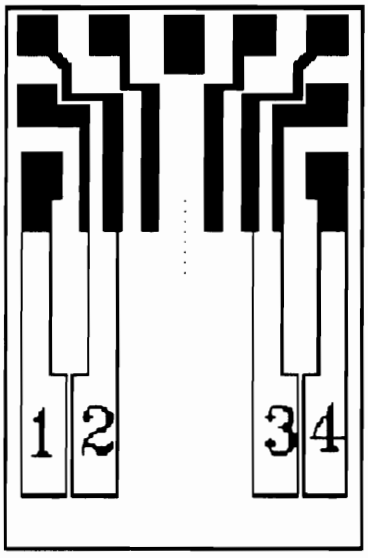

Figure 27 Igfet with source and drain numbered

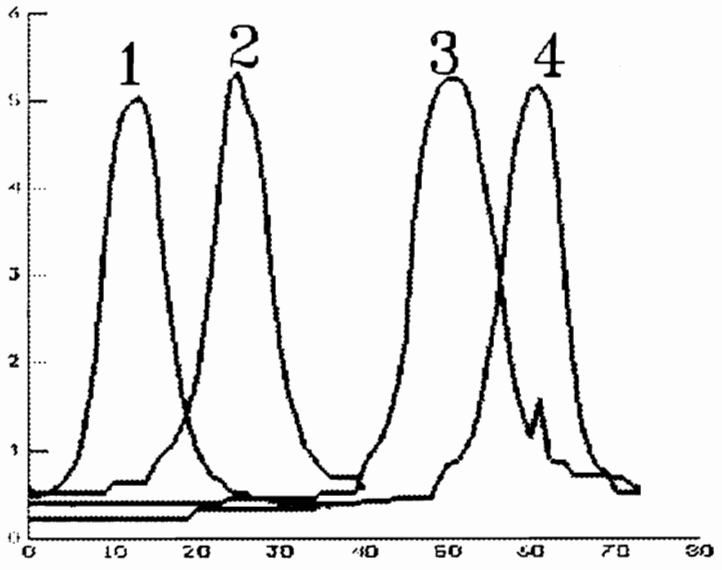

Figure 28 The experimental data

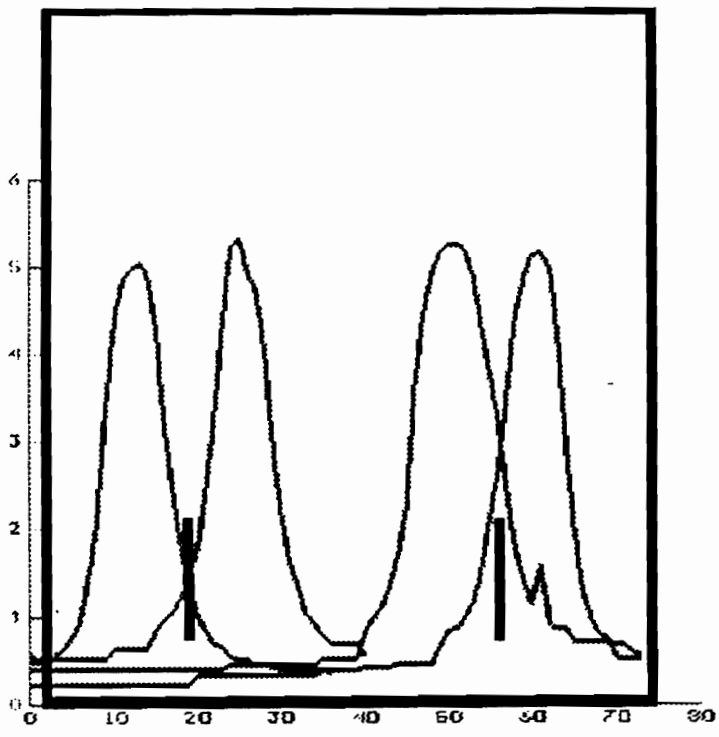

Figure 29 chip and data

4.3 Wavelength Response

Wavelength response is one of the main characteristics that must be considered when evaluating the IGFET as an optical sensor. To determine wavelength response the sensor was placed in an optical beam of known wavelength and photon flux and the current produced was measured. The photon flux is the number of photons in a cross sectional area of the light beam. Since the photon flux and the surface area of the sensor was known then the number of photons striking the sensor could be calculated. After the current was measured, then the ratio of electrons produced to photons striking the sensor was calculated. This ratio is the quantum efficiency of the sensor at that wavelength. The above process was repeated for the wavelengths of interest and quantum efficiency was plotted vs. wavelength.

The wavelength response for the IGFET was determined in the optical characterization lab in the Electrical Engineering Department at Virginia Polytechnic Institute and State University. The instrument configuration is shown in Figure 30.

The output of a GE Gemini 300 lamp was directed to the input of a Jarrel Ash Monospec 50 monochromator. The output of the monochromator was directed through a chopper to the sample area. A long wavelength pass filter was used for wavelengths above 540nm to filter lower orders from the monochromator.

The output of the sensor was connected to an EG&G Model 181 current to voltage converter and its output and the sync pulse from the chopper were fed to an EG&G Model 117 lockin amplifier. The output of the lockin amp was input to a Keithley 717 programmable electrometer. The output of the electrometer was fed

via an IEEE 488 bus to an IBM AT personal computer. Asyst software running on the IBM AT computer was used to control the system and collect data. The data was output as an ASCII file and input to Trimetrix's software package, Axum, for plotting.

A United Detector Technologies Solar Cell (#10822) was used as a reference. It has a surface area of $2cm^2$. It was calibrated against a NIST standard by ITT in Roanoke, Va. The relative quantum efficiency vs wavelength graph for the IGFET is shown in Figure 31. The data is listed in Table 2. This result supports the conclusion that the IGFET is operating as a photodiode since the shape of its wavelength response curve shows the broad peak at about 560nm which is characteristic of a silicon photodiode as shown in Figure 32.

Consider the data shown in Figure 33. This figure is a plot of the data in Table 3 of response vs wavelength vs bias voltage. It was collected on a different IGFET with the same equipment shown in Figure 30. The wavelength response is about the same for bias voltages from -1 volts to +1 volts. The response drops off dramatically at 1.5 volts, but the shape of the response curve remains the same. This rules out reverse bias breakdown. Dr. E. Riad, an expert in photo sensors, reviewed this wavelength response data and comments that this data alone sets the device apart from a typical photodiode. She also states that there is no obvious explanation for the phenomenon. Research efforts to explore this device further will be forthcoming from collaborative studies undertaken between the Virginia Polytechnic Institute and State University Chemistry and Electrical Engineering Departments and the Chemistry Department at St. John Fisher College where the author will extend the present work.

TABLE 2 WAVELENGTH RESPONSE DATA

Wavelength	Relative Response	Wavelength	Relative Response
380.00	0.86	630.00	0.78
390.00	0.99	640.00	0.74
400.00	0.90	650.00	0.70
410.00	0.76	660.00	0.68
420.00	0.71	670.00	0.63
430.00	0.68	680.00	0.66
440.00	0.66	690.00	0.66
450.00	0.63	700.00	0.67
460.00	0.62	710.00	0.67
470.00	0.64	720.00	0.66
480.00	0.66	730.00	0.66
490.00	0.69	740.00	0.66
500.00	0.74	750.00	0.67
510.00	0.80	760.00	0.66
520.00	0.86	770.00	0.68
530.00	0.91	780.00	0.73
540.00	0.96	790.00	0.73
550.00	1.03	800.00	0.77
560.00	1.01	810.00	0.84
570.00	1.00	820.00	0.80
580.00	0.99	830.00	0.88
590.00	0.95	840.00	0.84
600.00	0.93	850.00	0.63
610.00	0.88	860.00	0.87
620.00	0.84		

TABLE 3 WAVELENGTH RESPONSE AT LISTED BIAS VOLTAGES

WAVELENGTH	-1	-.5	0	.1	.5	1	1.5
360	661	577	608	740	703	635	459
370	739	673	633	781	733	647	419
380	586	563	530	651	626	535	339
390	529	522	472	562	545	474	298
400	509	493	483	565	542	498	298
410	526	479	542	624	589	572	344
420	448	443	445	493	484	456	274
430	446	445	448	490	485	461	266
440	482	481	477	537	520	494	283
450	595	576	614	704	675	644	362
460	563	571	558	607	600	571	331
470	645	654	637	680	679	649	378
480	723	735	712	756	754	723	421
490	798	811	790	827	831	797	457
500	840	856	834	868	874	839	482
510	844	867	835	872	879	843	486
520	823	845	818	848	856	822	476
530	775	797	769	793	801	775	444
540	712	732	701	723	730	705	407
550	724	714	702	749	755	730	392
560	626	626	610	635	746	627	344
570	565	578	552	575	580	565	310
580	528	537	517	529	542	530	292
590	483	493	466	487	493	482	268
600	496	501	486	495	504	496	277
610	462	470	453	465	473	463	255

TABLE 3 (CONT.) WAVELENGTH RESPONSE AT LISTED BIAS VOLTAGES

WAVELENGTH	-1	-.5	0	.1	.5	1	1.5
620	466	472	455	461	470	463	257
630	464	472	451	461	449	458	257
640	465	472	454	463	454	459	260
650	470	479	454	466	459	461	263
660	473	481	455	472	462	462	259
670	441	452	422	439	428	432	238
680	497	498	481	493	479	484	275
690	515	521	497	514	497	503	284
700	541	548	520	532	524	523	301
710	563	573	547	553	544	550	315
720	591	592	566	581	572	569	325
730	588	579	587	608	591	596	357
740	619	617	620	634	621	626	369
750	647	656	651	656	648	656	370
760	654	655	662	657	645	659	389
770	720	705	700	713	696	705	407
780	771	758	751	759	745	756	438
790	800	786	783	803	782	787	482
800	828	834	825	809	802	834	478
810	887	878	866	847	859	879	533
820	866	847	844	829	832	852	513
830	867	855	870	896	848	874	496
840	906	883	906	890	888	878	568
850	904	878	874	863	843	865	549
860	879	845	852	858	828	829	512

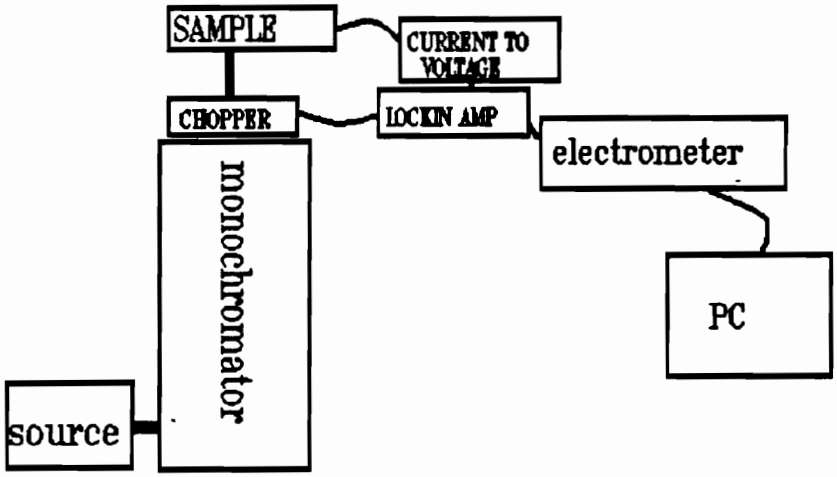

Figure 30 Wavelength response instrumentation

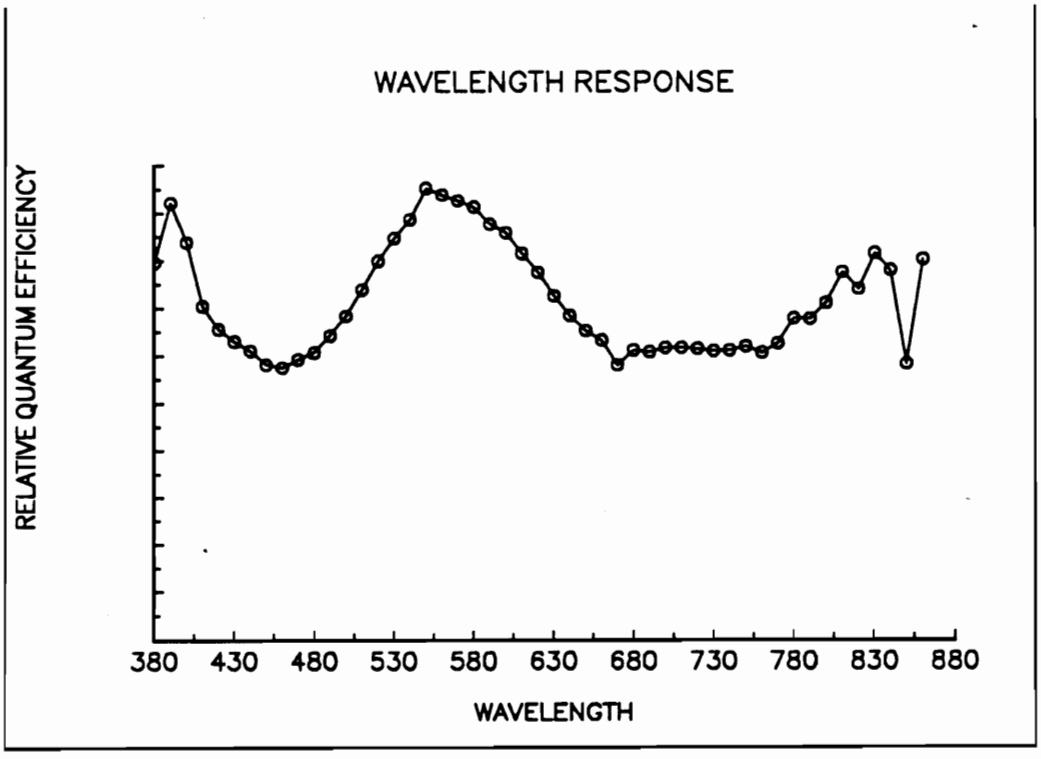

Figure 31 Optical - Wavelength response

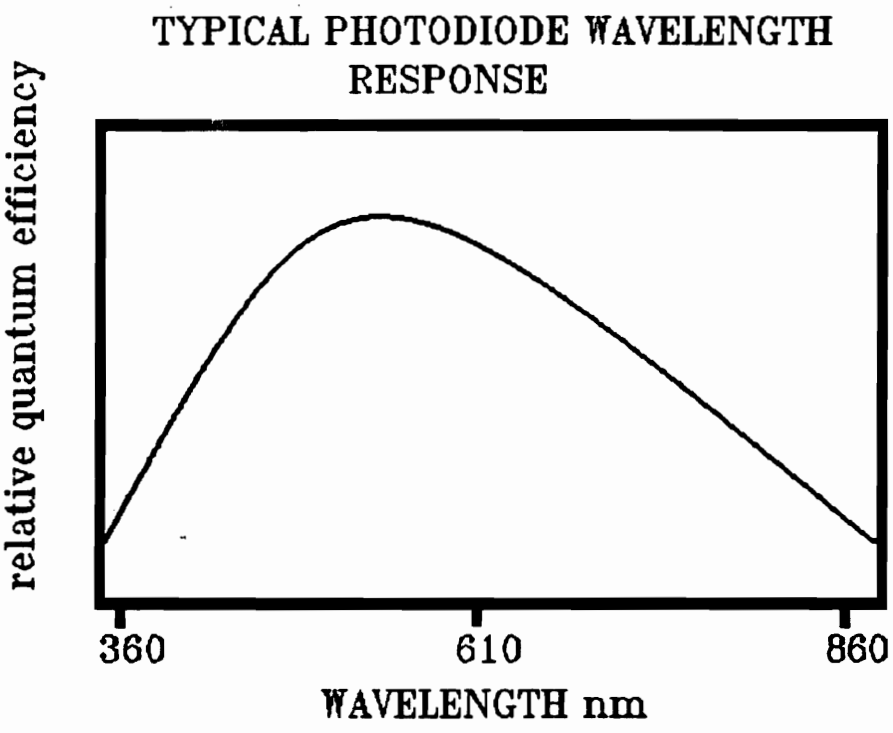

Figure 32 Wavelength response for silicon photodiode (97)

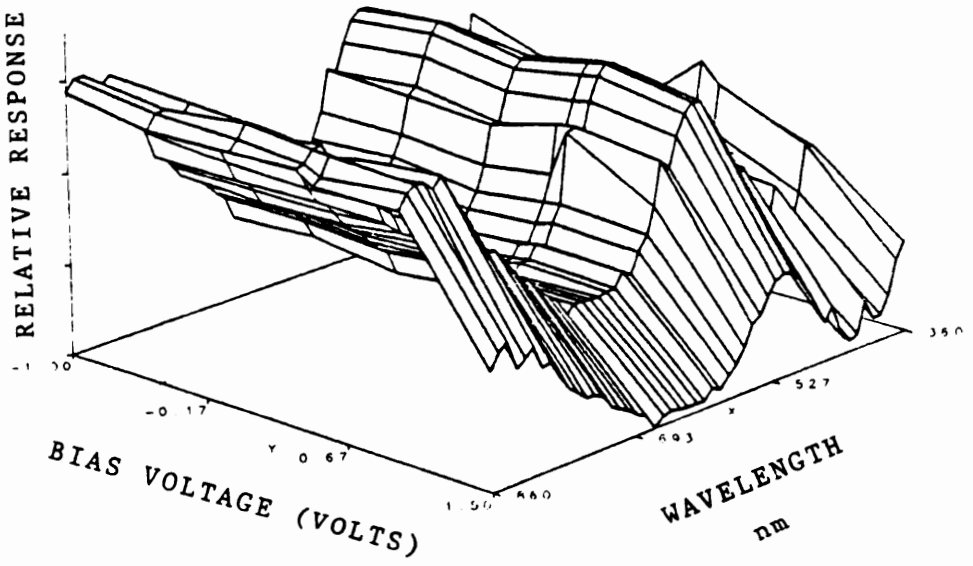

Figure 33 Response vs. Wavelength vs. Bias Voltage

5. THE INITIAL EXPERIMENT

5.1 Equipment

After realizing the IGFET is light sensitive, a device was built to make an initial determination if it is sensitive enough to be of interest as a microluminometer. The 2mm * 1.25mm chip was glued to a sixteen leg gold plated substrate and wirebonds made as described in Chapter 4 and shown in Figure 23. The integrity of the bonds was checked by standard tension tests.

A highly fluorinated monomer, Figure 34, was used with a siloxane crosslinking agent, Figure 35, as the epoxy to attach the flowcell and encapsulate the wirebonds and the rest of the chip insulating them from chemical contact with the environment. These compounds were obtained from Dr. Jim Griffith at the Naval Research Labs (98). The epoxy was prepared by mixing 2.1 grams of the monomer with 0.3 grams of the cross-linking siloxane in a capped test tube. Care was taken to expose the siloxane to the atmosphere for a minimum time in order to avoid carbon dioxide absorption. The test tube was mixed vigorously for 15 seconds in a vortex mixer. The tube was then clamped in a vertical position with the lower half immersed in an oil bath at 55 $^{\circ}$C. A magnetic stirbar was used to mix the liquids while they were in the oil bath. Initially the mixture was cloudy but became clear after about 20 minutes in the oil bath. The test tube was heated for 40 minutes.

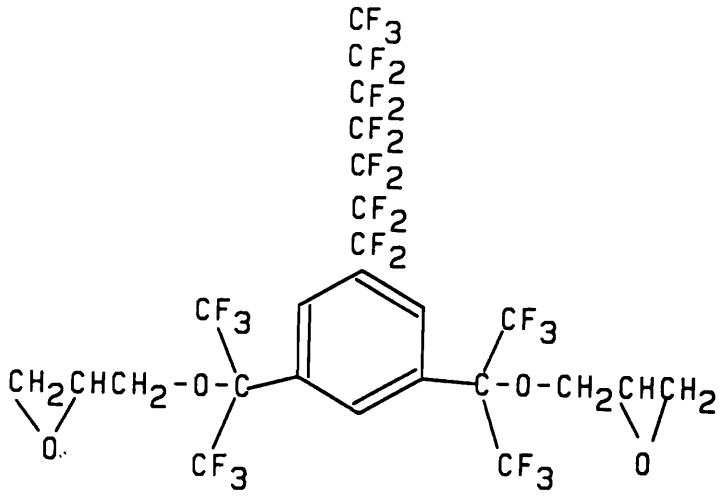

Figure 34 Highly fluorinated monomer

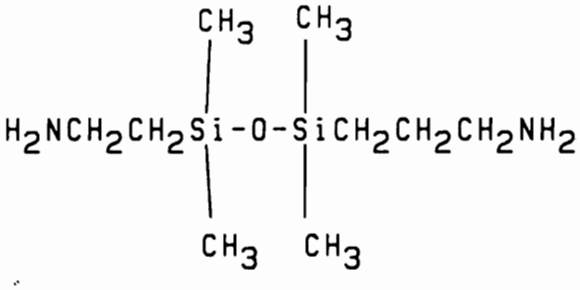

Figure 35 Crosslinking agent

The surface mount device with the attached and wirebonded chip was placed on a heated stage at 60°C under a field microscope. Micromanipulators were used to position the flowcell, as shown in Figure 36, and hold it in place while epoxy was pipetted around the flowcell, filling the well of the surface mount device and covering the rest of the chip and wirebonds. The device was kept on the heated stage for one hour and then transferred to an oven at 60°C for 24 hours.

The flow cell was made in the Chemistry Department Glass Shop at Virginia Polytechnic Institute and State University by Mr. F.M. VanDamme. The cell had a volume above the chip of approximately one microliter. The open area at the bottom of the flow cell was approximately 0.5mm x 1 mm. The flow cell is pictured in Figure 37.

The flowcell-chip-surfacemount assembly was attached to the test platform with a Plexiglass holder designed to press the legs on three sides of the surface mount device to the gold traces on the test platform. The legs on the fourth side were not used and a slot was cut in the Plexiglass holder to allow it to fit around the flow cell. The Plexiglass holder can be seen in Figure 37. It was held in place by four screws.

A Plexiglass housing was built to hold the test platform and protect the extremely fragile flowcell. The test platform in the Plexiglass housing is shown in Figure 38 with a later modification for a syringe stop.

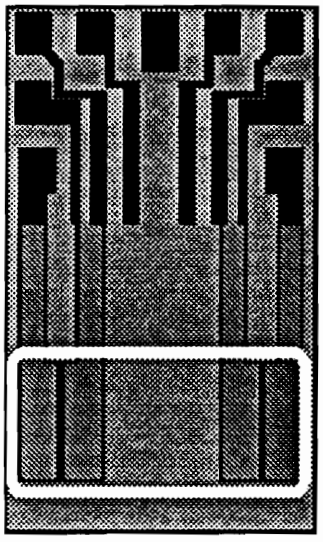

Figure 36 Flow-cell position on the IGFET

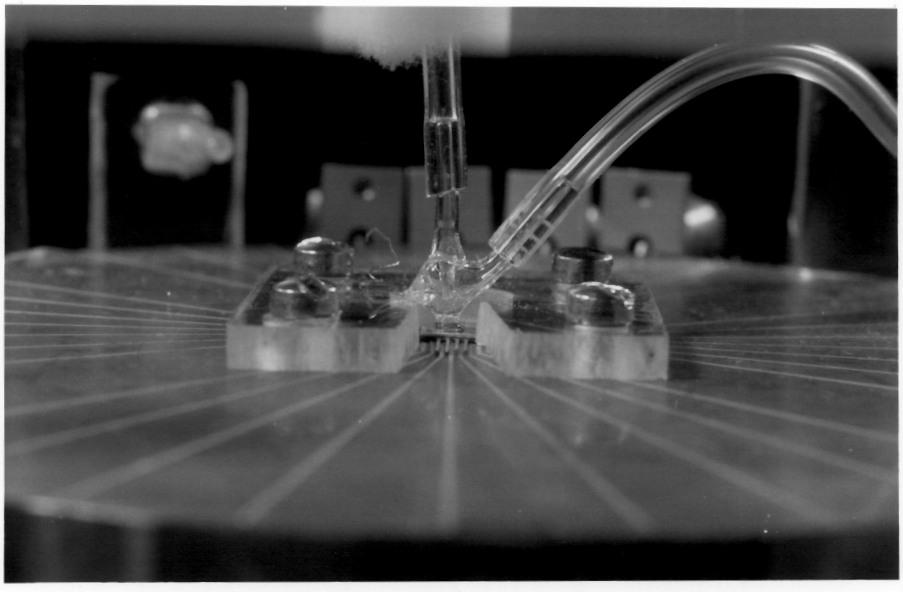

Figure 37 Glass Flowcell

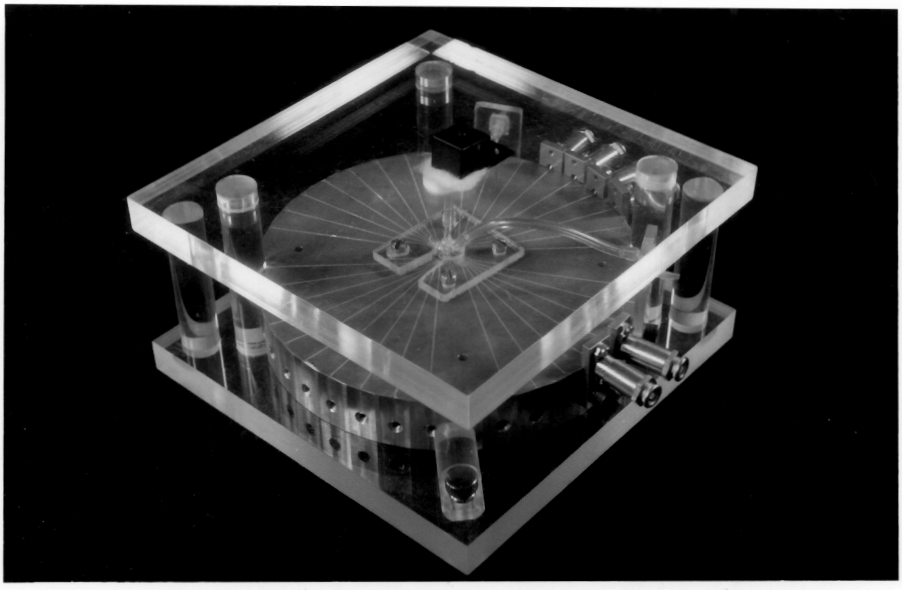

Figure 38 Plexiglass Housing

The Plexiglass holder with the test platform installed was placed in a black metal container with cover to prevent ambient light effects. Holes were drilled to allow access for wires and tubes. The initial reaction was done using a small reactor built by cutting the end off a plastic 5ml vial and connecting an "L" shaped tube connector. This allowed .1 ml volume reactions to be performed. The reactants were pumped through the flowcell by a peristaltic pump at the other end as shown in Figure 39. The experiments performed with this system are reported in the results section of this chapter.

Next, the system was modified to allow microliter quantities of reagents to be pipetted directly into the flow cell. To this end a hole was cut through the top of the Plexiglass shield and an aluminum syringe stop was constructed and mounted above the hole. A piece of tubing was connected to the flowcell and fed straight up through the hole in the Plexiglass through a hole in the syringe stop. This allowed a GC syringe to be inserted into the tube such that when the glass body of the syringe hit the syringe stop the bevel of the syringe was in the flow cell but could not strike the chip. Now microliter quantities of reactants could be syringed into the cell and reacted just above the chip. The Plexiglass shield with the syringe stop installed on top is shown in Figure 38. Figure 40 shows the black enclosure with a microliter syringe.

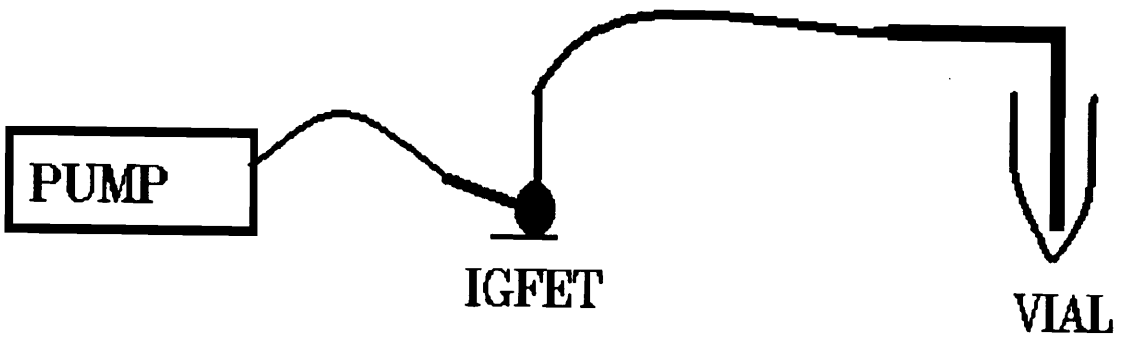

Figure 39 Initial system

Figure 40 Black metal enclosure with syringe

5.2 Results

The first experiment run was intended to gain a rough feel for the suitability of the IGFET as a microluminometer. This involved the firefly luciferin/luciferase system for adenosine triphosphate, ATP. The firefly system is one of the most efficient and best known chemiluminescent reactions. Quantum efficiencies of greater than 90% have been reported. ATP, luciferin, or luciferase can be directly measured with this reaction. $Lambda_{max}$ for the reaction is 562nm. The reaction is shown in Figure 41

The luciferin, luciferase, potassium arsenate, and magnesium sulfate mixture (FLE-50) and the ATP was obtained from Sigma. The FLE-50 vial was reconstituted with 5.0 ml of HPLC grade H_2O. A 0.1 ml aliquot of the FLE-50 reagent mixture was pipetted into the microreactor and $2 * 10^{-7}$ moles of ATP was added by pipetting 0.1 ml of a $2 * 10^{-3}$M ATP solution. A peristaltic pump drew the reaction mixture through the flow cell at a rate of 10 ml/min. Figure 42 shows the output for $2 * 10^{-7}$ moles of ATP. The amplifier was set on 0.1 nanoamps full scale.

This initial result was most encouraging. The hardware configuration was modified to allow the reaction to take place closer to the chip, which allowed smaller amounts of reactants to be used. The modified configuration, described above in the equipment section, allowed reagents to be micropipetted directly into the flow cell. A GC syringe was used to pipet 1 microliter of the luciferin/luciferase mixture and 1 microliter of the $2*10^{-3}$M ATP solution into the flow cell. The signal output for $2 * 10^{-9}$ moles of ATP is shown in Figure 43. Since these initial results showed significant sensitivity to light from a luminescent reaction, a more detailed implementation of the IGFET as a microluminometer was pursued.

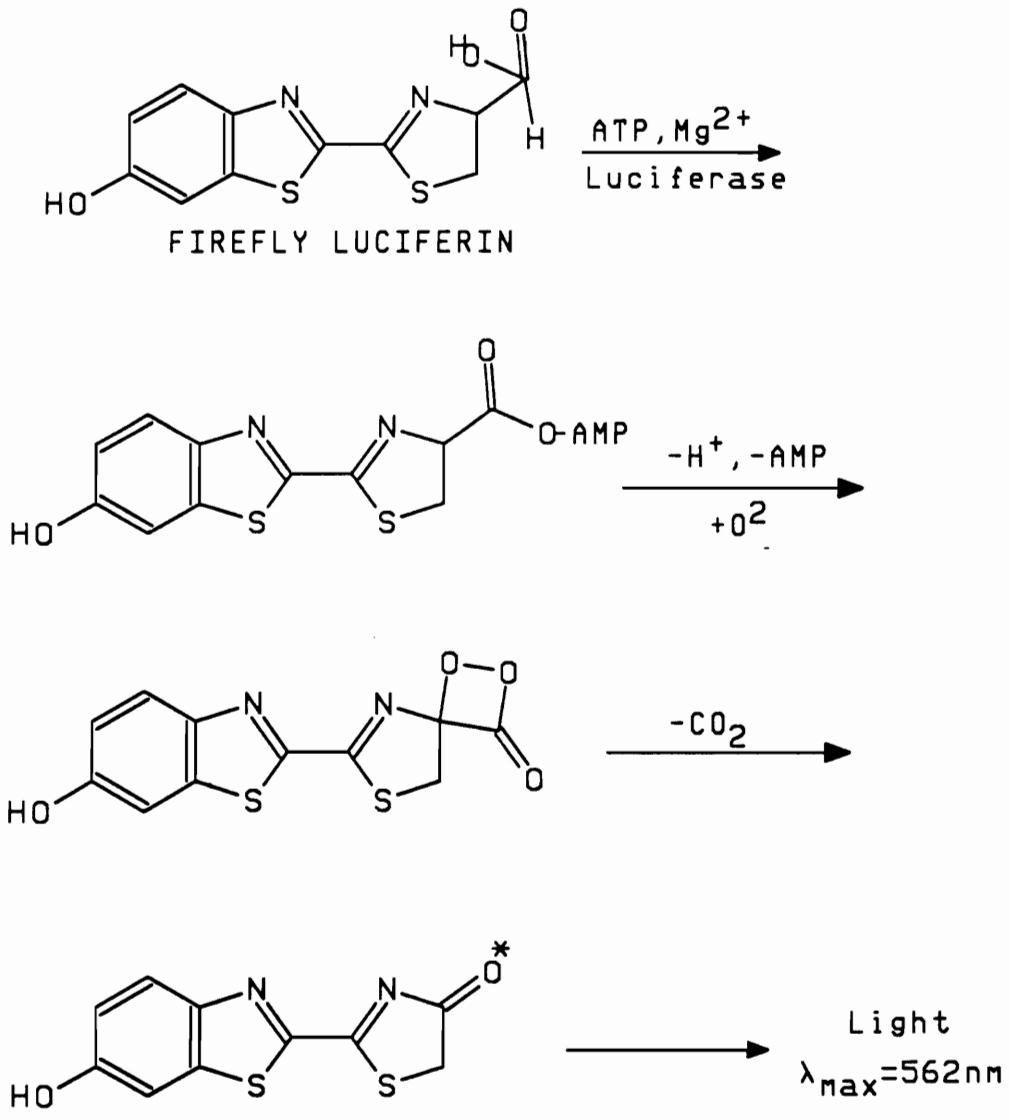

Figure 41 Firefly Luciferase System

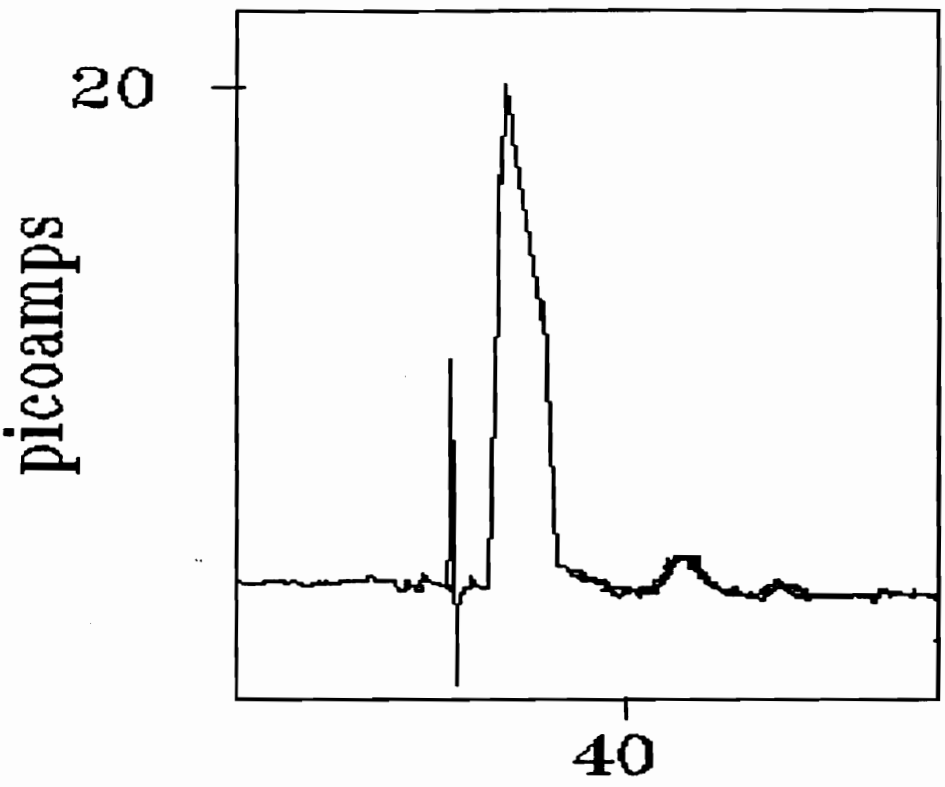

Figure 42 $2 * 10^{-7}$ moles ATP

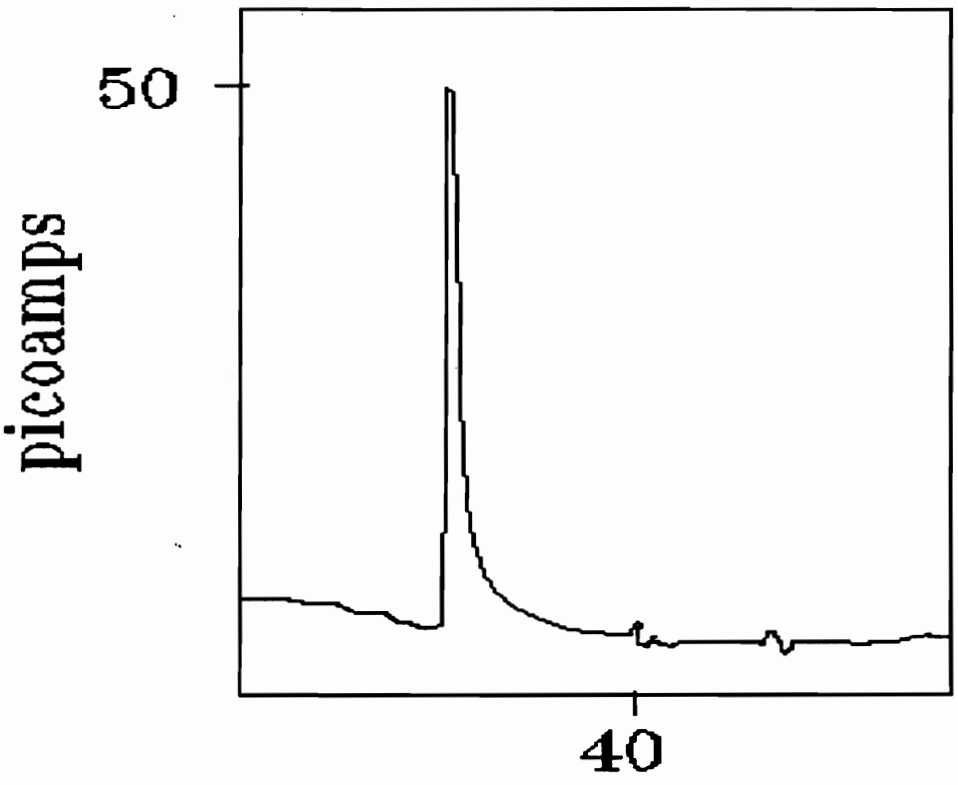

Figure 43 $2 * 10^{-9}$ moles ATP

6. DETECTION OF RECAEQUORIN

6.1 Introduction

Microluminometers have a strong future due, in part, to some exciting developments in the use of recombinant DNA techniques. The recombinant techniques allow the DNA fragment responsible for the production of the luminescent related proteins (Lux casette) in luminescent organisms to be inserted in another organism allowing that organism to express the pertinent proteins in high yield. An example of this work is the production of the photoprotein aequorin. Aequorin is a 22,000 dalton protein which emits blue light, $lambda_{max}$=469 nm, in the presence of calcium ion. Each mole of aequorin contains one mole of coelenterate luciferin which is required for light production. Light emission results from the reaction shown in Figure 44 (99).

In 1985 Cormier reported the production of aequorin by overexpression in E. coli of a DNA which was cloned from the jellyfish *Aequoria victoria* (100). Thus aequorin can be obtained by fermentation of the E. coli rather than having to tediously extract it from the jellyfish. The recombinant product is called recapoaequorin. Recapoaequorin is converted to recaequorin by incubation with synthetic coelenterate luciferin, dissolved oxygen, and a thiol agent.

Recaequorin is used as a tag for antibodies, proteins, and nucleic acids (101). The following work demonstrates the IGFET as a microluminometer for sensing recaequorin.

6.2 Experimental

50 micrograms of recaequorin was obtained from Dr. David Smith at the biochemistry department at the University of Georgia. This sample had been lyophilized from a 200ul pH 8 solution of 10mM Tris, 0.15M NaCl, 2mM EDTA and 0.1 mg/ml bovine serum albumin.

The 50 micrograms of aequorin was reconstituted in 0.5ml of 0.010M Tris, 0.15M NaCl, 0.002M EDTA at pH 8. This yielded a $4.6 * 10^{-6}$M solution of recaequorin. Dilutions were made with the above buffer with 0.1 mg/ml bovine serum albumin added.

A device for dispensing 0.1M calcium acetate solution was constructed by placing a 1/16" miniature barbed polypropylene tubing fitting into the end of 1/16" inside diameter tygon tubing. The tubing and connector were fastened to a 5.5" long 1/4" diameter Plexiglass rod using plastic wire ties. A rod and clamp system with a magnetic base was used to hold the dispenser in place above the chip. A Gilson Minipulse 2 peristaltic pump was used to dispense the solution. The variable speed control was set to give a flow rate of 0.3 ml/min. The base of the chip was connected to ground and one drain was connected to the input of the Keithley picoammeter.

The chip was mounted in the substrate as shown in Figure 4.4. The substrate was placed in the bottom of an empty black plastic 35mm film container. Holes were drilled in the bottom of the container for the wires leading from the substrate to the amplifier. The film container was clamped with a portable vise. During data collection black cloth was place over the top of the container and dispensing arm.

Data was collected by using a Hamilton #701 10 microliter syringe to pipet 6 microliters of aequorin solution onto the chip. The calcium acetate dispenser was placed just above the sample bead as shown in Figure 45.

The Data from the Keithly amplifer was collected using an Axon Instrument TL-1 DMA Interface connected to an IBM PC. A 13 point Savitsky-Golay digital filter and peak integration was performed on each run using Trimetrix's software product Axum. Between runs the chip was rinsed with deionized water and acetone and placed in a 60° oven for 5 minutes. An example of the peak shape is seen in Figure 46 which shows a plot of the data for 0.28 picomoles of recaequorin. The results shown in Table 4 are plotted in Figure 47. The line drawn in Figure 47 is the regression for the points listed in Table 4.

6.3 Limit of Detection (LOD)

R^2 for the regression line in Figure 47 is 0.9986. Other workers have found recaequorin gives a multidecade linear response (102).

Long and Winefordner (91) have suggested using 3 times the standard deviation of blank measurements divided by the analytical sensitivity, i.e., the slope of the regression line, to calculate the limit of detection. The standard deviation of the blank measurements was calculated to be $2.366*10^{-4}$ area units. The sensitivity was 11544 area units/picomoles. According to the above method the LOD is $6*10^{-20}$ moles of recaequorin. This makes the IGFET microluminometer analytically useful for recaequorin detection.

6.4 Discussion

In a recent study to develop a diagnostic assay for salmonellae antigen, recaequorin was used as a tag in the bioluminescent immunoassay (BLIA) (103). All of the results reported fell well above the IGFET's LOD for recaequorin. They used thirty times the reagent volumes used above and they employed an expensive photomultiplier based luminometer.

The food industry has a strong need for field testing of their products for salmonellae antigen. The development of a portable method is strongly sought. A portable test would avoid the time and expense of sending samples to laboratories. The expense of purchasing a luminometer limits the acceptance of luminescent based techniques by the food industry.

Developing an IGFET based assay for salmonellae antigen would provide the food industry with an onsite method of testing without the expense of purchasing an expensive luminometer and smaller volumes of reagents would be required. Imagine having a system similar to home based glucose testing systems with reagents immobilized on strips. In this case the IGFET would be part of the structure of the strip with reagents immobilized on it. As more luminescent reagents are developed by recombinant DNA and other techniques the demand will increase for complementary microluminometers for the development of new inexpensive portable techniques for determination of a multitude of analytes.

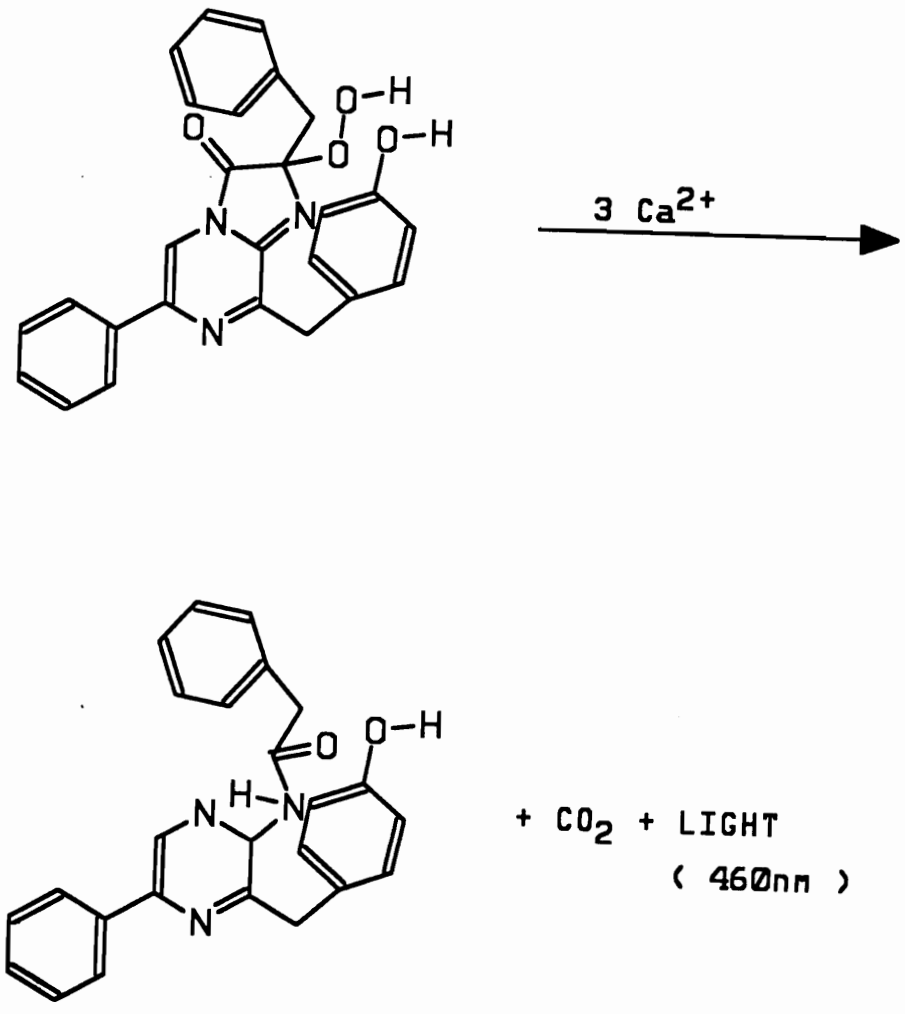

Figure 44 Aequorin reaction with Ca++

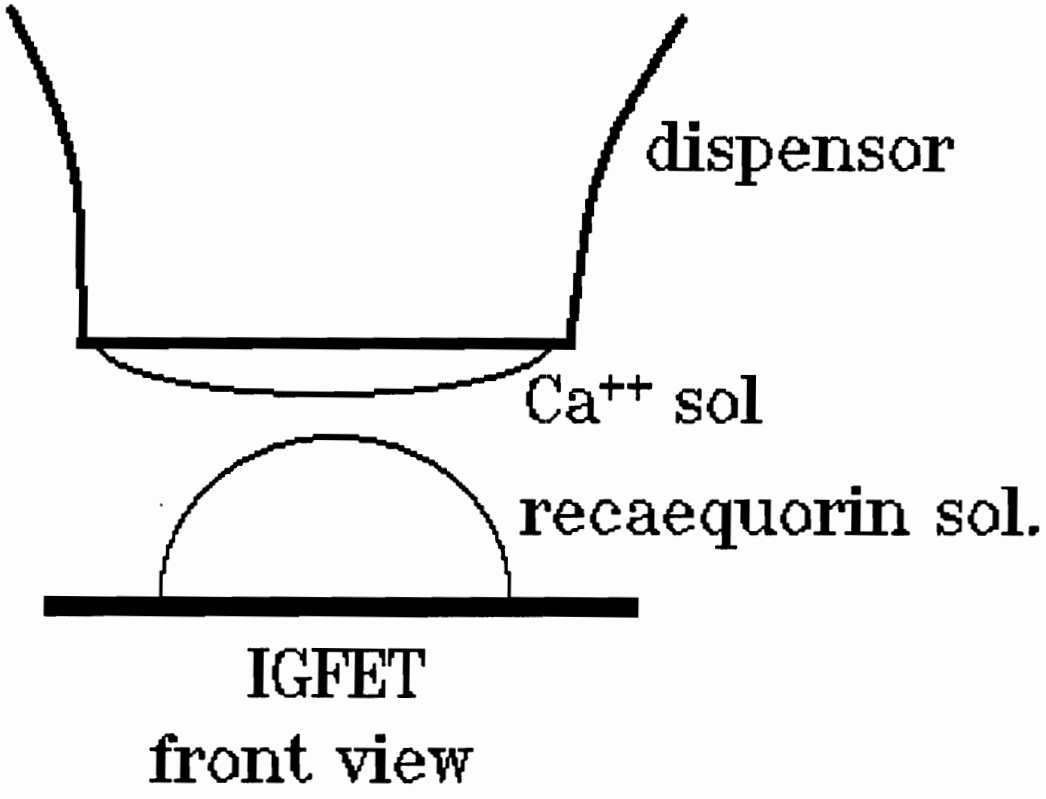

Figure 45 Ca++ dispenser above recaequorin sample on IGFET

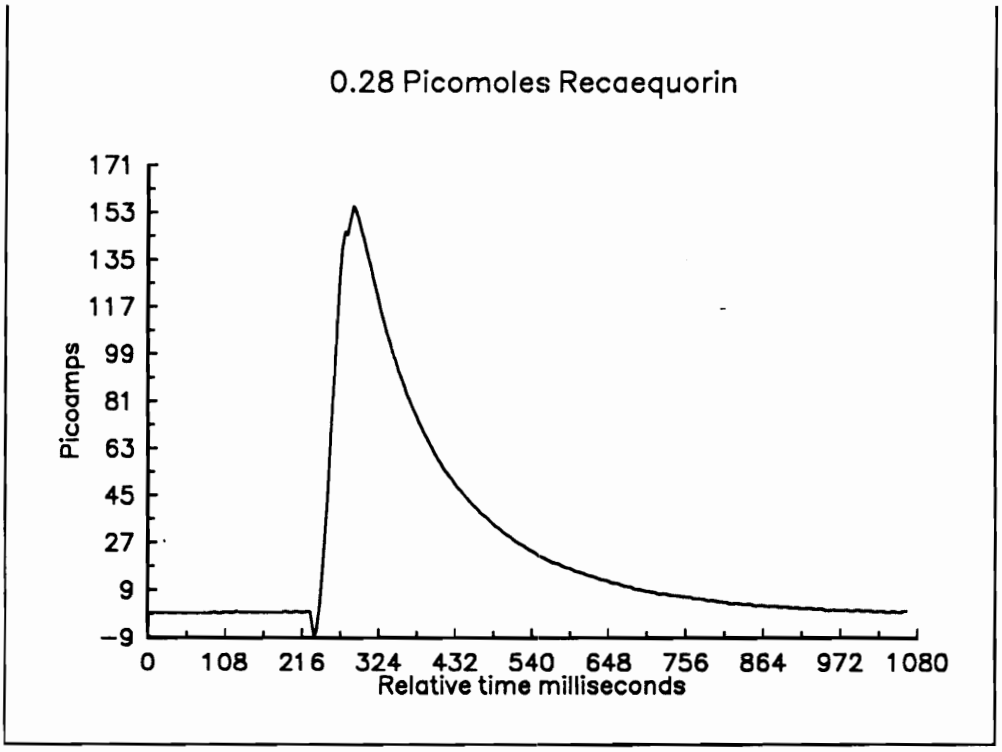

Figure 46 The peak for 0.28 picomoles recaequorin

Table 4 Recaequorin Calibration Data

Picomoles Recaequorin	Area Units
0.28	6351
2.80	45000
7.00	81163
14	164532
28	330000

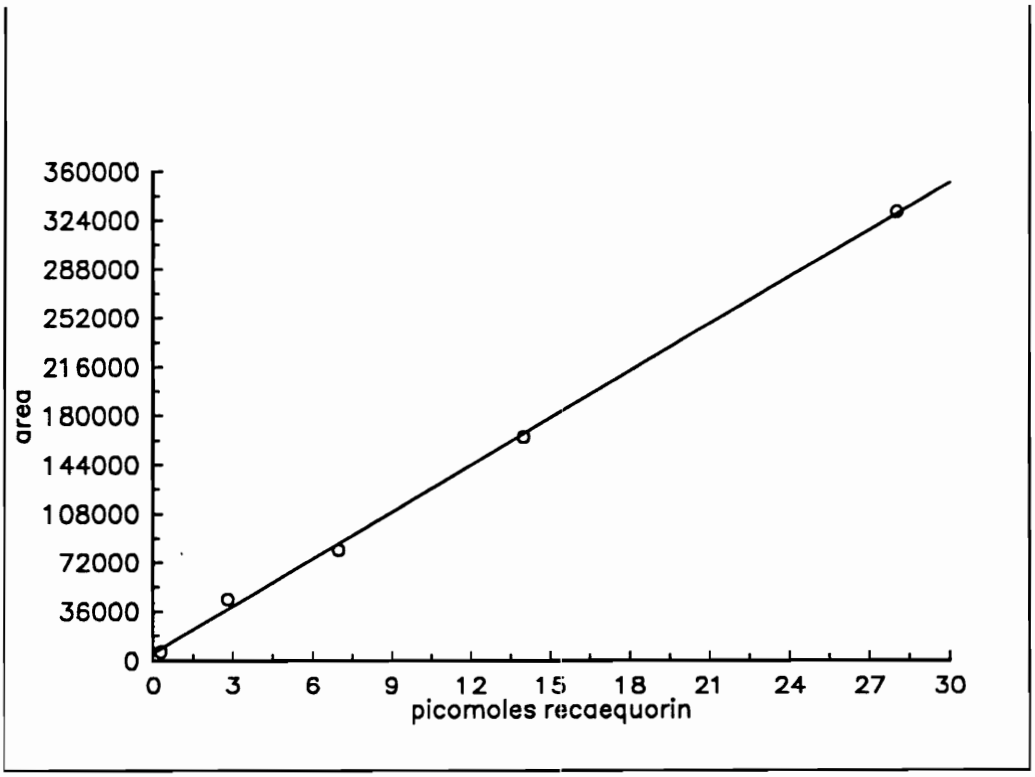

Figure 47 Recaequorin Calibration curve

7. AN IGFET BASED FLOW INJECTION CHEMI-MICROLUMINOMETER

7.1 Equipment

An automated flow system was constructed as shown in Figures 48 and 49. The equipment described in Chapter 5 was used as the basis for the FIA system. Instead of injecting sample manually with a syringe an air actuated sample valve (104) injected 16 or 25 microliters of sodium hypochlorite solution into a tee connector where it mixed with the luminol solution 8.5cm above the flow cell. Figure 50 shows the automated injection valve above the black enclosure. The reagents were pumped by peristaltic pumps. The system was controlled by an IBM personal computer (PC) interfaced to a Perkin Elmer robotics device interface.

Data from the IGFET was collected via a Keithly micromicroammeter, which gives a 0-5V output. This output was input to an analog to digital convertor into an LSI-ll microcomputer. The PC triggered the LSI-11 to begin data collection. The LSI-11 determined the peak maximum and sent this data to the IBM PC via a serial interface. The LSI-11 was operated as a satellite to a host DEC 11/23. PolyForth was used on the LSI-11 and the Perkin-Elmer robot control language PERL was used on the PC. Axum and SAS were used on the PC and IBM mainframe respectfully for plotting and analyzing data. Software listings are in the appendix.

7.2 Results

The sodium hypochlorite/luminol system was used with the automated flow injection microluminometer system to show the feasibility of using the IGFET as a detector in a microluminometer FIA system. This work demonstrates the use of the sensor as a quantitative luminometer for a chemiluminescent reaction. The luminol (5-amino-2,3-dihydro-1,4-phthalazinedione) reaction is shown in Figure 51. Quantum yield is defined as the number of photons produced per molecule reacting. The quantum yield for luminol reactions is about 1%. Chemiluminescent systems characteristically have lower quantum yields than bioluminescent systems. $Lambda_{max}$ for the light given off by the luminol reaction is 562nm. The luminol system is widely used for chemiluminescence determinations (105). The oxidation of luminol by hypochlorite was first described by Albrecht (106). Early use of this reaction for the determination of hypochlorite was by Ponomarenko (107) and later by Babko (108).

Even though luminol is one of the best known chemiluminescent compounds, there is no agreed mechanism for the light emitting step in luminol reactions (109,110). Seitz notes that a one electron oxidation of luminol yields an intermediate radical, while a two electron oxidation of luminol yields an azaquinone intermediate. Since hypochlorite oxidizes via a two electron step, then the azaquinone intermediate is likely for the reaction between hypochlorite and luminol, as shown in Figure 52. The azaquinone intermediate can then react with either oxygen (first order process) or hypochlorite (second order process) as shown in Figures 53 and 54 respectively (110). Marino and Ingle found that purging the

luminol solution with nitrogen to remove oxygen had no effect on luminescent signals (111). Therefore no attempt was made to adjust the dissolved oxygen level in the solutions used. The kinetics of this system is pseudo-first order in hypochlorite in the presence of excess luminol. The system gave a linear response for the points with luminol in excess by a least a factor of ten. As the concentration of hypochlorite approaches the concentration of luminol then the calibration curve starts to level off as also reported by Marino and Ingle (111).

Figure 55 shows the response surface for 16 microliter injections of different concentrations of sodium hypochlorite at flow rates ranging from 3.5 mls/min to 27 mls/min. SAS grid was used to create a response surface from the data points in Table 5 and SAS graphics were used to plot the response surface. The sodium hypochlorite solutions were produced from a 5% stock solution. The stock solution was standardized by sodium thiosulfate titration (112,113). The luminol concentration was 0.068M in 0.1M NaOH.

Since the luminol solution is 0.06M the points for .006M, .0006M and .00006M hypochlorite were used for the calibration curve. The calibration curve for a flow rate of 27ml/min is shown in Figure 56 based on the data in Table 6.

7.3 Limit of Detection

R^2 is 0.999 for the regression line drawn with the calibration data in Figure 56. The LOD was determined as described in chapter 6. The standard deviation for five blanks was 0.0947 picoamps. The sensitivity is 11.35 picoamps/nanomole ClO^-. The LOD is calculated to be $25 * 10^{-12}$ moles hypochlorite. This is six times better than the LOD of $160 * 10^{-12}$ moles hypochlorite reported recently for a

FIA spectrophotometric method for ClO^-(114). The literature also reports a three decade linear range. No direct comparison of this system to another FIA luminol/ClO^- can be made because none was found in the literature. The reports found for determination of hypochlorite by luminol chemiluminescence were either static systems using ml quantities of sample (111) or they were continuous flow systems using relatively huge quantities of sample (65mls/min) (115).

7.4 Throughput

The throughput for the FIA IGFET based microluminometer is 720 samples per hour at a reagent flow rate of 27ml/min. Literature reported throughput values (in samples per hour) were 90 (111), 70 (114), and 80 (116).

7.5 Future

Future work in this area will involve further optimization of the FIA IGFET microluminometer. Much work can be done with different flow cell design incorporating mixing of the sample and reagent closer to the detector. Incorporating an integrating sphere type flow cell would be of interest. It is also of interest to totally automate the system for temperature, pH, reagent and sample flow rate, sample size, and reagent and sample concentration. Then software can be written to optimize a given parameter, e.g., limit of detection or throughput. Once this system is functional then different luminescent systems can be characterized.

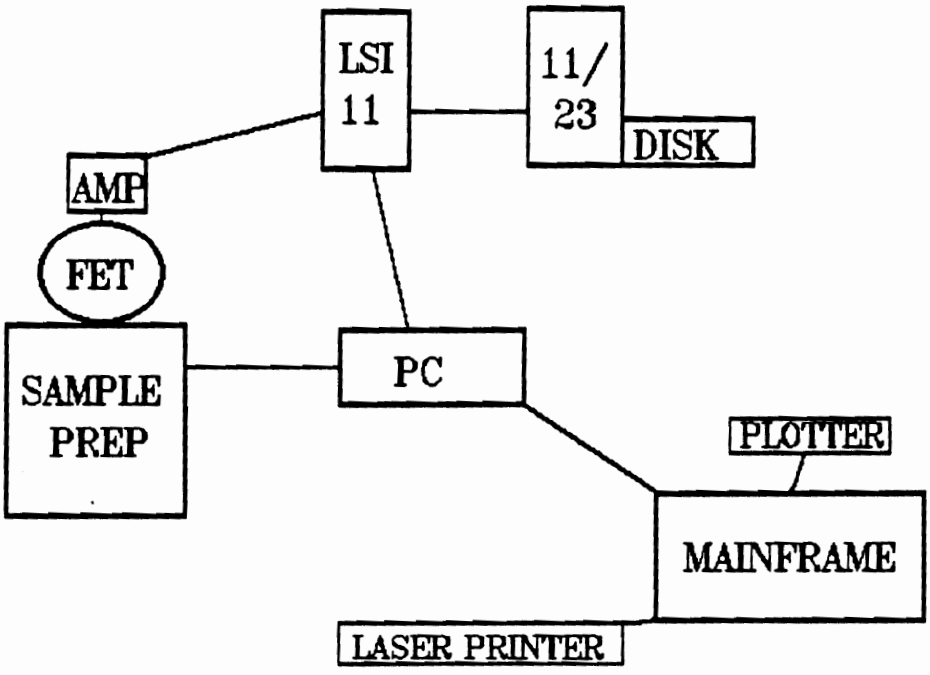

Figure 48 Hardware overview

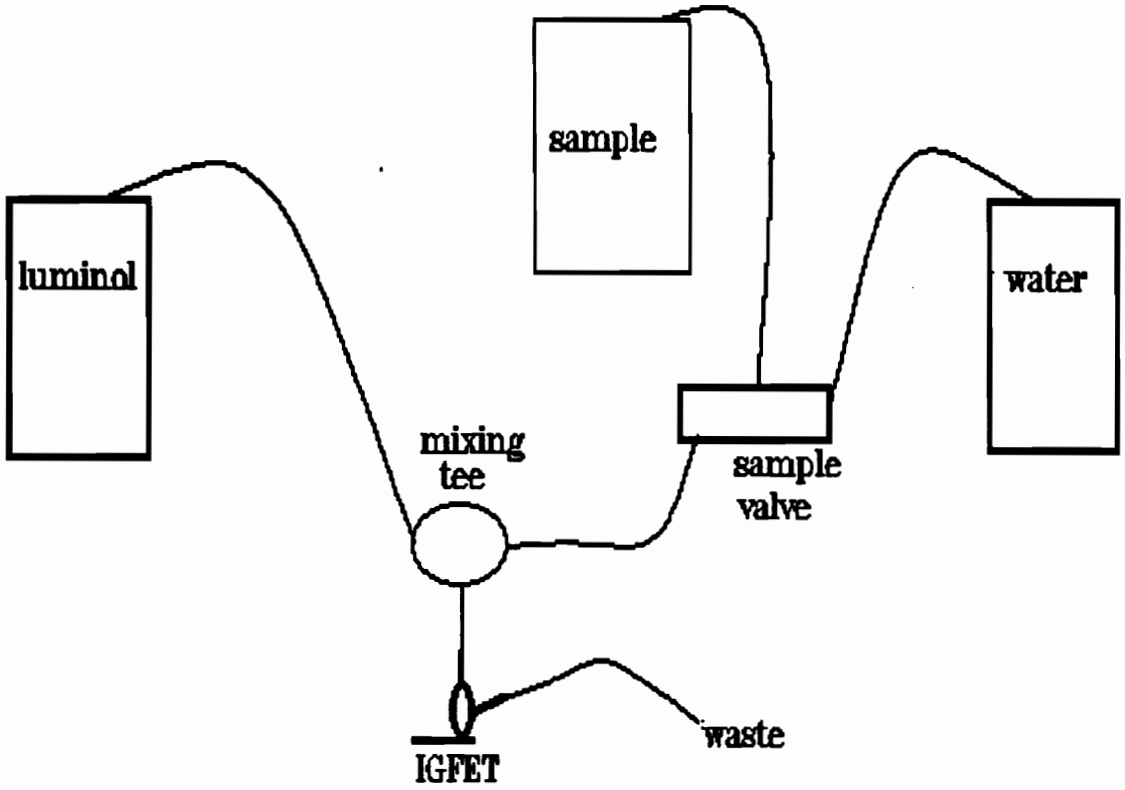

Figure 49 The flow system

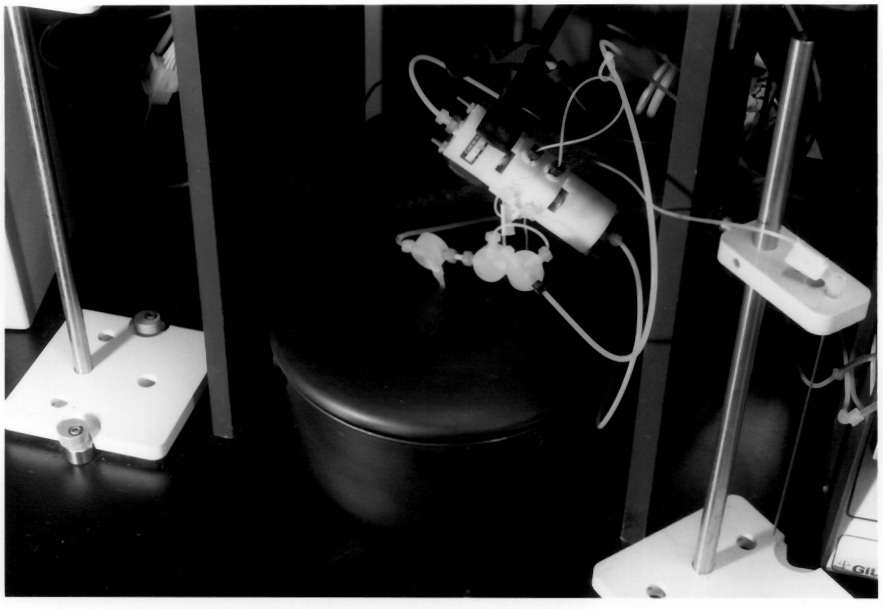

Figure 50 Automated injection system

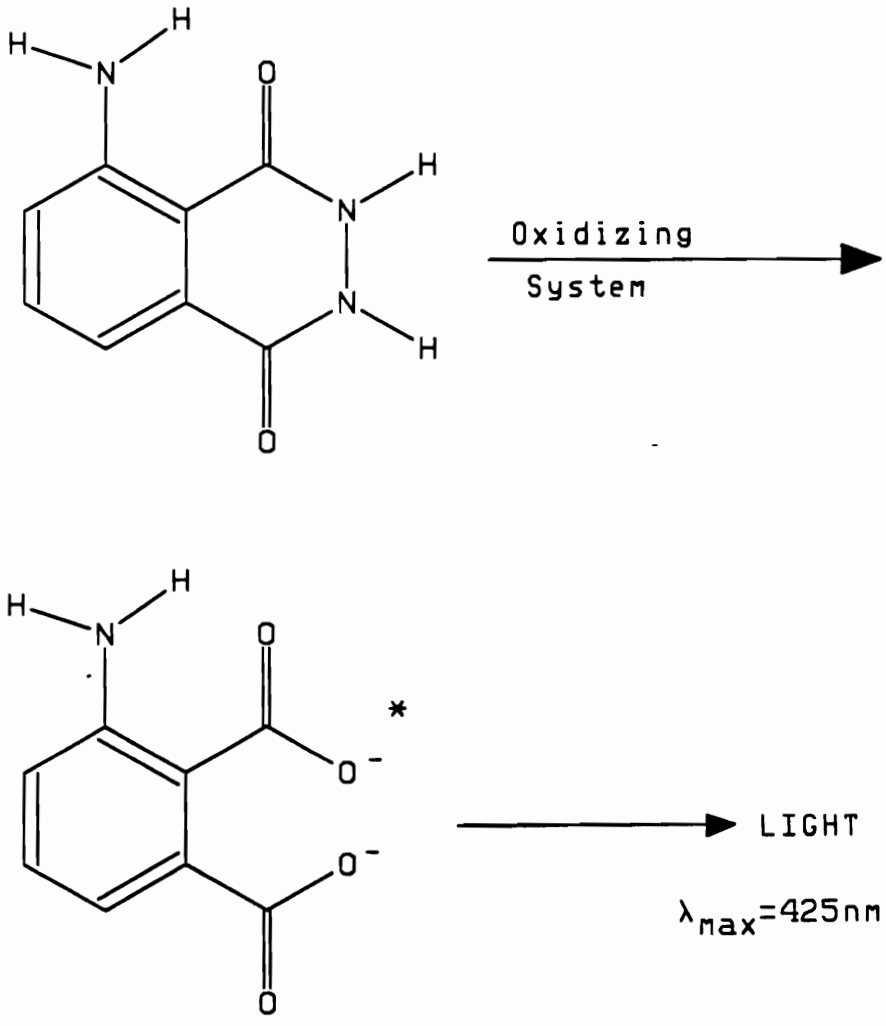

Figure 51 Luminol Reaction

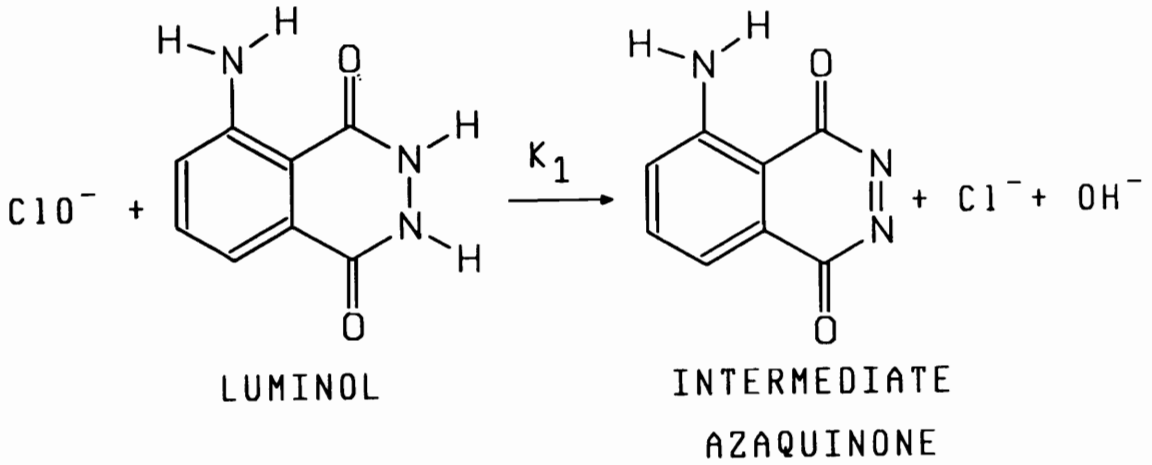

Figure 52 The first step of the Luminol Hypochlorite Reaction

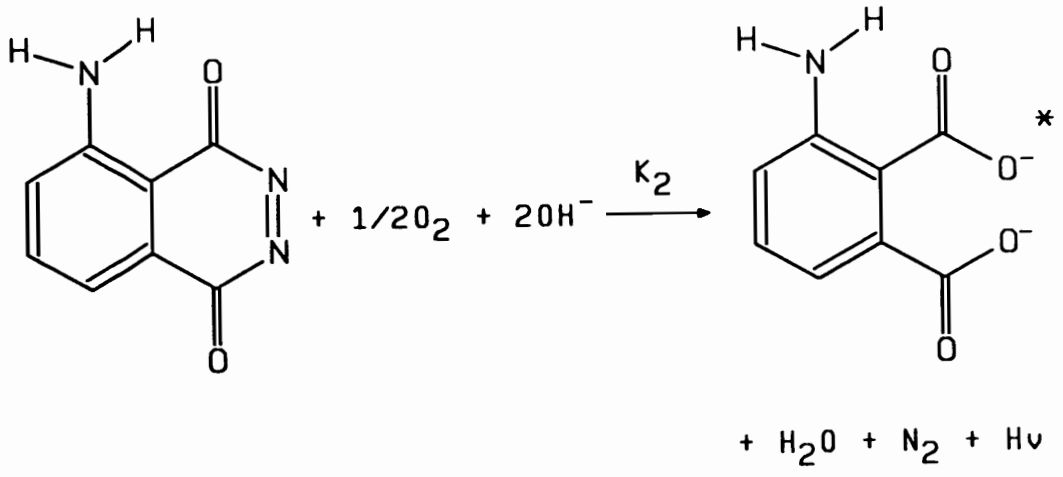

Figure 53 Azaquinone reaction with oxygen

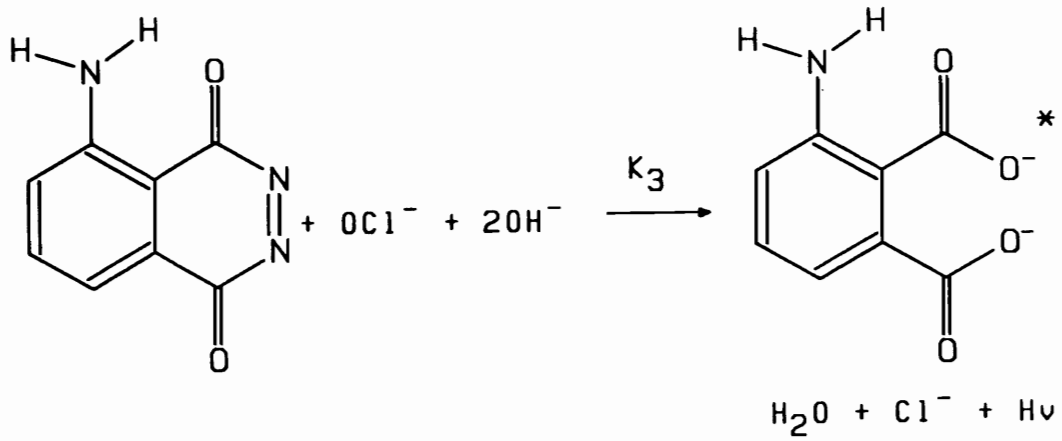

Figure 54 Azaquinone reaction with hypochlorite

Table 5 Response Surface Data

960 nanomoles hypochlorite

mls/min	27	20	8.5	7	3.5
	2090	1810	1107	678	398
	2132	1814	1157	681	393
	2102	1832	1129	659	394
	2099	1804	1107	678	374
		1806			
mean	2106	1813	1125	674	390

96 nanomoles hypochlorite

	1109	1012	989	649	433
	1085	1010	1006	646	424
	1082	1010	987	650	463
	1074	1014	961	601	426
	1078		964	601	416
mean	1086	1011	981	629	432

9.6 nanomoles hypochlorite

mls/min	27	20	8.5	7	3.5
	111	110	92.56	64.21	37.84
	112	110	94.24	64.04	37.04
	110	110	95.70	65.28	35.96
	111	109.5	92.20	63.16	36.18.7
				65.80	36.405
mean	111	110	93.7	64.5	36.7

Table 5 cont. Response Surface Data

0.96 nanomoles hypochlorite

mls/min	27	8.5	3.5
	13.11	12.87	12.62
	12.92	12.84	12.50
	13.18	12.82	12.48
	12.87	12.70	12.62
	12.99	12.79	12.35
mean	13.0	12.8	12.5

Nanomoles	Flow mls/min	Picoamps
960	3.5	390
960	7	674
960	8.5	1125
960	20	1813
960	27	2106
096	3.5	432
096	7	629
096	8.5	981
096	20	1011
096	27	1086
9.6	3.5	36.7
9.6	7	64.5
9.6	8.5	93.7
9.6	20	110
9.6	27	111
.96	3.5	12.5
.96	8.5	12.8
.96	27	13.0

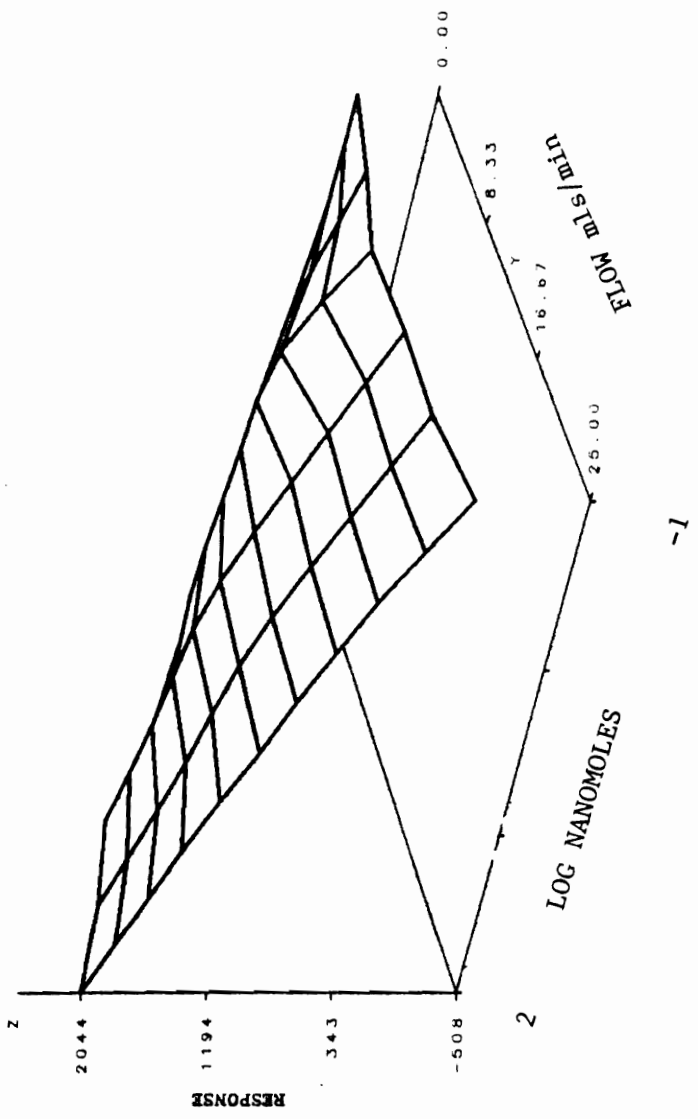

Figure 55 Response surface for IGFET FIA microluminometer luminol/hypochlorite system

Table 6 Calibration data for the luminol hypochlorite reaction

Nanomoles	0.96	9.6	96
Picoamps	13.1	111.0	1109
	12.9	112.0	1085
	12.9	110.5	1082
	13.2	111.2	1074
	13.0		1078
Mean	13.0	111.2	1086
Std. Dev.	0.13	0.64	13.7
RSD	1.0%	0.62%	1.26%

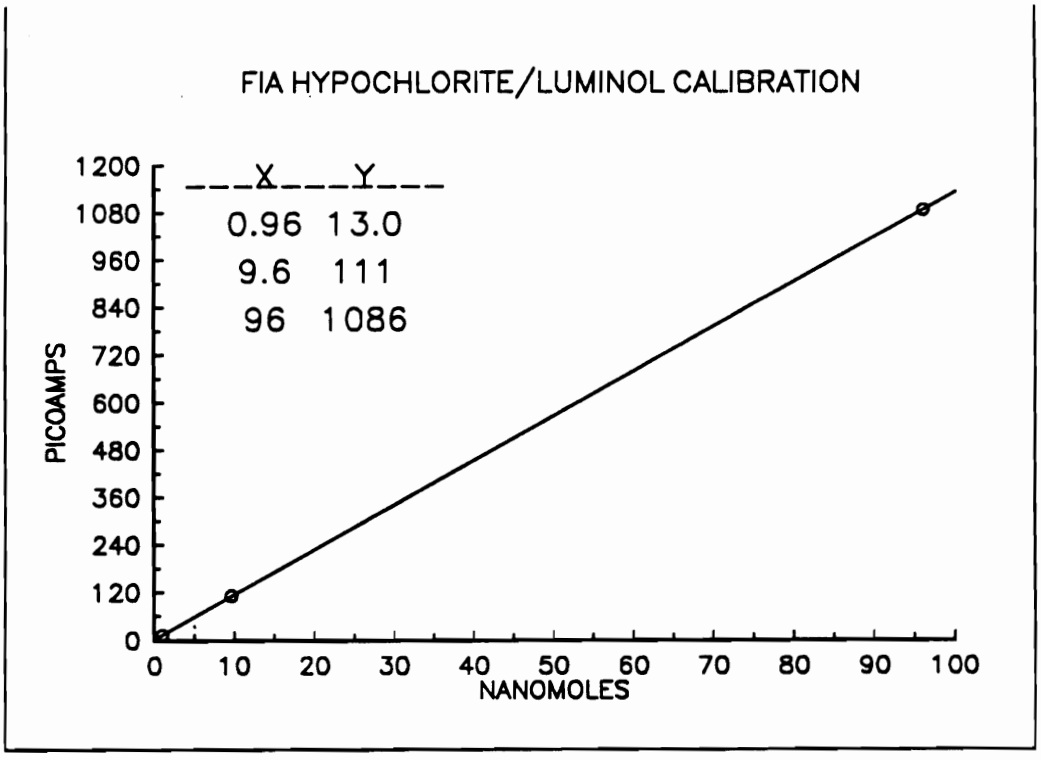

Figure 56 Calibration curve for luminol/ClO^-

7.6 Immobilized Enzyme

To demonstrate the feasibility of enzyme enhancement of the microluminometer system an enzyme was immobilized and placed near the chip's surface. The hydrogen peroxide - peroxidase - luminol system was used. Peroxidase was immobilized on nylon filament using glutaraldehyde (117).

The last 8mm of a 3cm segment of .2mm diameter Nylon 6 filament was placed in 4M HCl at room temperature for 10 minutes to hydrolyze the surface. After three rinses in deionized water the segment was placed in 12.5% (w/v) solution of glutaraldehyde in .01M sodium borate buffer for thirty minutes at 4 °C. The segment was rinsed three times with sodium borate buffer and placed in a solution of Sigma type VI 275 units/mg peroxidase. The peroxidase was dissolved in 5 ml of .1M, pH 7.0 phosphate buffer and $2.5 * 10^{-5}$M EDTA. The nylon was placed in the enzyme solution for 16 hours at 4 °C. The segment was rinsed three times with 0.2M NaCl solution to remove unbound enzyme. The segment was stored in 0.1M phosphate buffer at 4°C until it was used. Figure 57 shows the structure formed between Nylon 6 and peroxidase with glutaraldehyde.

A 3% stock solution of hydrogen peroxide was standardized by titration with sodium thiosulfate (112,118). 25 microliters of an aqueous 1 to 10 dilution of the stock solution (0.25 micromoles) of hydrogen peroxide was injected six times into 0.003M luminol in .1M NaOH and the average result was calculated and normalized to 1. Then the 3cm nylon filament segment with immobilized peroxidase was placed in the flow cell resting on the IGFET as shown in Figure 58.

Five micromoles of hydrogen peroxide was injected six times and the average result was calculated and normalized, giving a result of 1.27. Thus the immobilized enzyme gave a 27% enhancement over the no enzyme case.

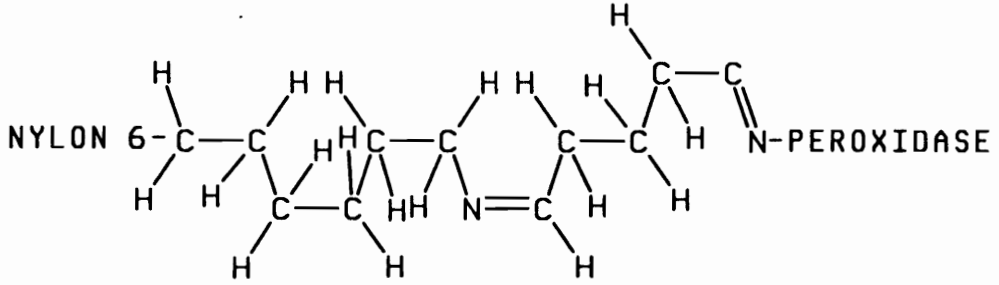

Figure 57 Peroxidase immobilized on Nylon 6 with Glutaraldehyde

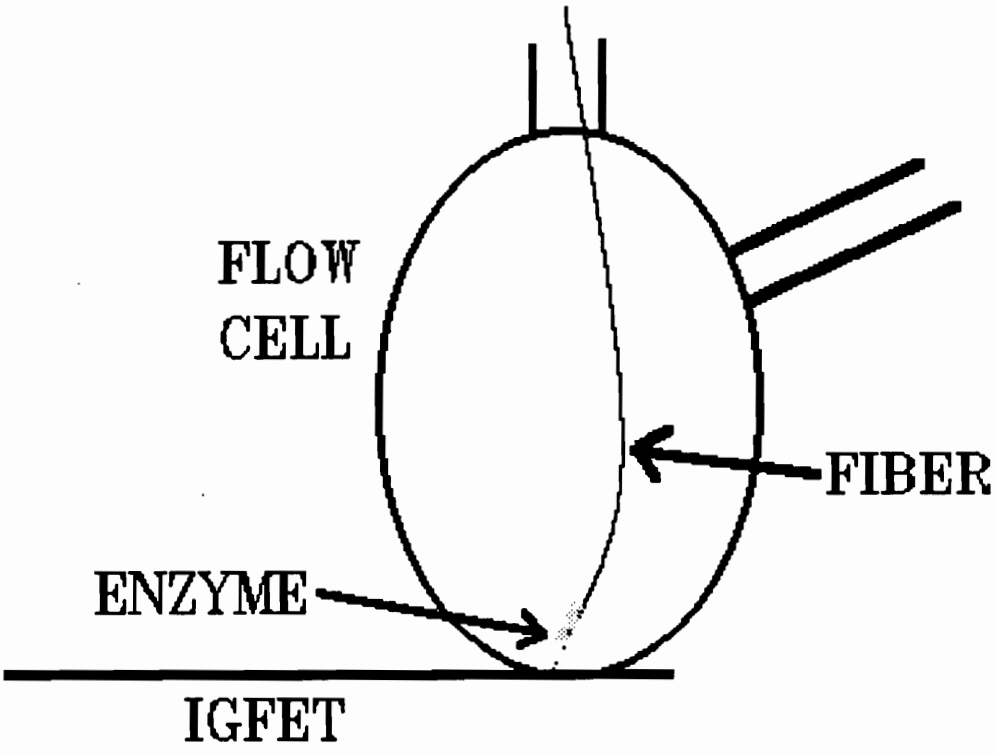

Figure 58 Nylon fiber in the flow cell

8. CONCLUSION

This work shows the feasibility of using the IGFET as a microluminometer. The IGFET has traditionally been used as an ion sensing device. It is most interesting to study a device from a different perspective than its traditional use. The first question we had in considering the IGFET as an optical sensor was is it sensitive enough for it to be of interest? We have answered that question. It is.

The next question was how does it work. This work has demonstrated that the light sensing is independent of the traditional operation of the field effect transistor. Light sensing involves the source or drain but not the gate. Light does not regulate current from source to drain. The cynic at this point might say, well then, it's just acting as a photodiode and of what interest is that?

First, consider the wavelength response. The IGFET has broader useful wavelength response than the photodiode.

Second, consider the data shown in Figure 33. This data shows response vs wavelength vs bias voltage. As mentioned earlier, Dr. Elshabini Riad, an expert in photo sensors, reviewed this wavelength response data and comments that this data alone sets the device apart from a typical photodiode. She also states that there is no obvious explanation for the phenomenon.

Third, consider the size of the IGFET. A typical photodiode used as a luminometer is $6mm^2$ (119). The light sensitive area of an IGFET is $0.007mm^2$. This makes it an ideal candidate for a synergistic relationship with fiber optic sensors (3). This would eliminate the need to expand the optical output from a fiber to cover the surface of a larger photodiode. The IGFET can be placed within a few

microns of the end of the fiber or even attached to the fiber. With larger core fibers, >100 microns, the IGFET can be used to study the flux density. The instrument built in this study that used a 4 micron core fiber to probe the chip with photons can be adapted for this purpose. Instead of having a 4 micron core fiber in the chuck, the larger fiber would be mounted. The IGFET would be moved across the output of the fiber and the intensity vs position in the diameter of the fiber would be recorded.

Finally, consider the geography of the chip. It has two insulated gate transistors and two MOSFET's. This gives the opportunity for using one of the IGFET's as a traditional ion sensor, the drain of the other IGFET as a microluminometer, and the MOSFET's in a circuit of choice. For example, an amplification circuit. This offers the opportunity to perform ion sensing and photon sensing on the same piece of silicon. Or one IGFET can be multiplexed between ion sensing and photon sensing by using a digitally controlled analog multiplexer to switch the IGFET from a circuit for measuring response to photons to a circuit for measuring response to ions. Another option for utilizing the unique layout of the chip is for two point photon sensing in a kinetic study. A capillary tube in an FIA system can be placed across the chip so it crosses both IGFET's. Then, for example, the drain of each IGFET can be used to sense light from a reaction taking place in the tube as the reactants move through the tube. Since the distance between the drains is known, then reaction kinetics occurring in a sample bolus can be determined. For a fast luminescent reaction the light output at two different distances from the mixing point can be obtained. A variation on this would be to place micro optical interference filters over each drain or put two different wavelength LED's on the other side of the column. This would allow monitoring

the absorbance of the material flowing through the column at two wavelengths. This would be a micro version of Dr. Dave Hooley's Ph.D. work at Virginia Tech (120, 121).

An exciting opportunity for silicon micromachining is to combine ion sensing and photon sensing in one 3 dimensional device. Imagine that the floor of the room you are in is an IGFET. The gate is a long narrow strip in the center of the room. On either side of the gate is the source and drain. The walls are pSi with a wallpaper covering of nSi. A new luminescent biomaterial is immobilized in the volume of the room. A large hole is cut in the wall on each end of the long narrow room. Tubes are connected to these holes and solution flows through the room. When analyte is carried into the room by the solution it reacts with the immobilized biomaterial and light is produced. The walls of the room sense the photons. The floor of the room senses the pH of the solution. A new biosensor is born. The technology to achieve this exists today (122).

The future for microluminometers is strong. In addition to the type of recombinant work done to produce recaequorin in which a recombinantly modified microorganism is used to produce a photoprotein by fermentation, recombinant techniques have been used to make new luminescent organisms. For example, the lux gene cassette from the microorganism *Vibrio fischeri* has been inserted into a naphthalene catabolic plasmid in *Pseudomonas fluorescens* (123). The modified organism luminesced after exposure to naphthalene. A new generation of biomaterials will result from these recombinant techniques and with it a growing demand for new and versatile microluminometers to complement them.

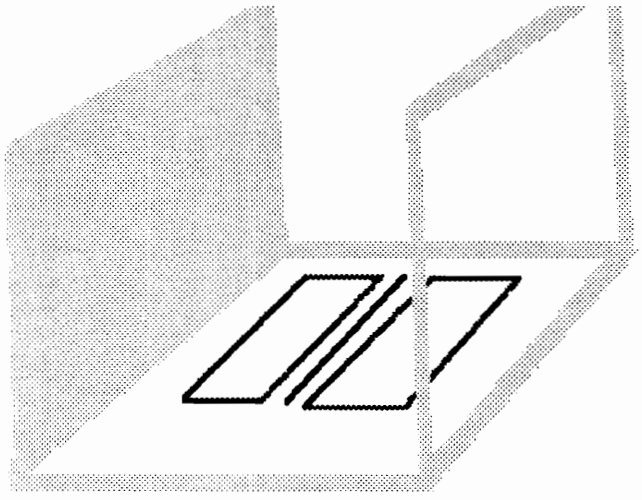

Figure 59 3D Biosensor

REFERENCES

1. Bergveld, P. *IEEE Trans. Biomed. Eng.* **1970**, 17, 70.

2. Blackburn, G. in *Biosensors*, Turner, A., Ed.; Oxford Unversity Press: Oxford, 1987; Chapter 26.

3. Dessy, R. E. *Anal. Chem.* **1989**, 61, 1070-94A.

4. Janata, J.; Huber, R. *Solid State Chemical Sensors*, Academic Press: Orlando, 1985.

5. Bergveld, P.; Sibbald, A. in *Comprehensive Analytical Chemistry*, Svehla, G. Ed.; Elsevier: Amsterdam, 1988; volume 23.

6. Janata, J. *Chem. Rev.* **1990**, 90, 691-703.

7. Janata, J.; Huber, R. *Ion-Selective Electrode* **1979**, 1, 31-79.

8. Bergveld, P. *Med. & Biol. Eng. & Comput.* **1979**, 17, 655-661.

9. Smith, R. L.; Collins, S. D. *IEEE Trans. Electron Devices* **1988**, 35(6), 787-789

10. Moody, G. J.; Slater, Jonathan M.; Thomas, J. D. R. *Analyst* **1988**, 113(1), 103-108.

11. Slater, Jonathan M. *Anal. Proc.* **1989**, 26(3), 96-98.

12. Wong, Hon Sum; White, Marvin H. *IEEE Trans. Electron Devices* **1989**, 36(3), 479-487.

13. Skowronska-Ptasinska, M.; Sudhoelter, E. J. R.; Reinhoudt, D. N. *Sens. Actuators* **1989**, 18(3-4), 309-327.

14. Comte, P.A.; Janata, J. *Anal. Chim. Acta* **1978**, 101, 247-252.

15. McBride, P.T.; Janata, J. *J. Bioeng.* **1978**, 2, 459-462.

16. Wang, Guihua; Yu, Dun; Wang, Y. *Bandaoti Xuebao* **1988**, 9(3), 235-243.

17. Wang, Guihua; Yu, Dun; Wang, Y. *Sens. Actuators* **1987**, 11(3), 221-237.

18. Barabash, Peter R.; Cobbold, Richard S. C.; Wlodarski, Wojciech B. *IEEE Trans. Electron Devices* **1987**, 34(6), 1271-1278

19. McBride, P; Janata, J.; Comte, P.A.; Moss, S.D.; Johnson, C *Anal. Chim. Acta.* **1978**, 101, 239-245.

20. Klein, M. *Sens. Actuators* **1989**, 17(1-2), 203-208.

21. Emde, C.; Hopert, R.; Riecken, E. O.; Neth. J. *Med.* 1989, 34(Suppl.), 3-9.

22. Liu, B. D.; Su, Y. K.; Chen, S. C. *Int. J. Electron.* **1989**, 67(1), 59-63.

23. Wong, Hon Sum; Hu, Yin; White, Marvin H. J. *Electrochem. Soc.* **1989**, 136(10), 2968-2967

24. Van den Vlekkert, H. H.; De Rooij, N. F. *Analusis* **1988**, 16(2), 110-119.

25. Van der Schoot, Bart; Bergveld, P. *Sens. Actuators* **1988**, 13(3), 251-256

26. Gotoh, Masao; Oda, Shunri; Shimizu, Isamu; Seki, Atsushi; Tamiya, Eiichi; Karube, I. *Sens. Actuators* **1989**, 16(1-2), 55-65.

27. Miyahara Shoichi; Murakami, Kenji; Yamamoto, T. *Shizuoka Daigaku Denshi Kogaku Kenkyusho Kenkyu Hokoku* **1987**, 22(2), 29-41.

28. Olthuis, W.; Van der Schoot, B. H.; Chavez, F.; Bergveld, P. *Sens. Actuators* **1989**, 17(1-2), 279-283.

29. Van den Vlekkert, H. H.; Kloeck, B.; Prongue, D.; Berthoud, J.; Hu, B.; De Rooij, N. F.; Gilli, E.; De Crousaz, P. *Sens. Actuators* **1988**, 14(2), 165-176.

30. Lee, Kwang *Man Nunmunjip Cheju Taehak* 1987, 25, 85-103.

31. Vogel, R.; Amaro, M.; Gaskill, R. *Proc. of the 1985 Int. Symp. on Microelectronics* **1985**, 490-493.

32. Oesch; U.; Caras, S.; Janata, J. *Anal. Chem.* **1981**, 53, 1983-1986.

33. Ito, Tadashi; Inagaki, Hazime; Igarashi, I. *IEEE Trans. Electron Devices* **1988**, 35(1), 56-64.

34. Chai, Zhiqin; Fang, Peisheng; Luo, J. *Kexue Tongbao* **1987**, 32(17), 1213-1216.

35. Wakida, Shinichi; Yamane, Masataka; Hiiro, K. *Bunseki Kagaku* **1989**, 38(3), 140-143.

36. Bezegh, Klara; Bezegh, Andras; Janata, Jiri; Oesch, Urs; Xu, Aiping;Simon, W. *Anal. Chem.* **1987**, 59(24), 2846-2848.

37. Thompson, John M.; Emmett, Christopher; Smith, Stephen C. H.; Cramb, Robert; Hutton, P. *Ann. Clin. Biochem.* **1989**, 26(3), 274-280.

38. Fang, Peisheng *Xi'an Jiaotong Daxue Xuebao* **1987**, 21(3), 95-101.

39. Wakida, Shinichi; Yamane, Masataka; Hiiro, Kazuo; Kihara, Teruaki; Ujihira, Yusuke; Sugano, T. *Anal. Sci.* **1988**, 4(5), 501-504.

40. Glavina, Paul G.; Harrison, D.; Jed C. J. *Chem.* **1987**, 65(5), 1072-1078.

41. Fang, Peisheng; Huang, Shunen; Zhou, J. *Fenxi Huaxue* **1989**, 17(1), 52-54.

42. Vegh, G.; Timar-Horvath, V. *Symp. Electron. Technol.* **1985**, 2, 217-223.

43. Tsukada, K.; Sebata, M.; Miyahara, Y.; Miyagi, H. *Sens. Actuators* **1989**, 18(3-4), 329-336.

44. Moritz, W.; Meierhofer, I.; Muller, L. *Sensors and Actuators* **1988**, 15, 211-219.

45. Van den Vlekkert, H.H.; De Rooij, N; Van den Berg, A.; Grisel, A. *Sens. Actuators* **1990**, B1(1-6), 395-400.

46. Locascio, Laurie E.; Janata, J. *Anal. Chim. Acta* **1987**, 194, 99-107.

47. Hu, B.; Van den Vlekkert, H. H.; De Rooij, N. F. *Sens. Actuators* **1989**, 17(1-2), 275-278.

48. Miyahara, Shoichi; Murakami, Kenji; Yamamoto, Tatsuo *Shizuoka Daigaku Denshi Kogaku Kenkyusho Kenkyu Hokoku* **1987**, 22(2), 29-41.

49. Moriizumi, Toyosaka; Sriyudthsak, Mana; Onoue, Y. *Hyomen* **1987**, 25(4), 242-245

50. Vogel, A.; Hoffmann, B.; Sauer, T.; Wegner, G. *Sens. Actuators* **1990**, B1(1-6), 408-411.

51. Battilotti, M.; Colilli, R.; Giannini, I.; Giongo, M. *Sens. Actuators* **1989**, 17(1-2), 209-215.

52. Oesch, Urs; Xu, Aiping; Brzozka, Zbigniew; Suter, Gabriela; Simon, W. *Chimia* **1986**, 40(10), 351-353.

53. Kleitz, M.; Million-Brodaz, J. F.; Fabry, P. *Solid State Ionics* **1987**, 22(4), 295-303.

54. Bataillard, P.; Clechet, P.; Jaffrezic-Renault, N.; Kong, X. G.; Martelet, C. *Sens. Actuators* **1987**, 12(3), 245-254.

55. Kampfrath, G.; Leimbrock, W. *Anal. Lett.* **1987**, 20(11), 1765-1767

56. Moody, G. J.; Thomas, J. D. R. *Analyst* **1988**, 113(11), 1703-1707.

57. Wong, A. S.; Michal, G. M.; Locci, I. E.; Cheung, P. W. J. *Mater. Res.* **1988**, 3(5), 1002-1009.

58. Harame, David L.; Bousse, Luc J.; Shott, John D.; Meindl, James D. *IEEE Trans. Electron Devices* **1987**, 34(8), 1700-1707.

59. Gimmel, P.; Gompf, B.; Schmeisser, D.; Wiemhoefer, H. D.; Gopel, W. *Sens. Actuators* 1989, 17(1-2), 195-120

60. Sibbald, A.; Shaw, J. E. A. *Sens. Actuators* **1987**, 12(3), 297-300.

61. Alegret, S.; Alonso, J.; Bartroli, J.; Bomenech, J.; Jaffrezic-Renault, N.; Duvault-Herrera, Y. *Anal. Chim. Acta* **1989**, 222(2), 373-377.

62. Alegret, S.; Alonso, J.; Bartroli, J.; Del Valle, M.; Jaffrezic-Renault, N.; Duvault-Herrera, Y. *Anal. Chim. Acta* **1990**, 231(1), 53-58.

63. Caras, S. and Janata, J. *Anal. Chem.* **1980**, 52, 1935-1937.

64. Hanazato, Yoshio; Inatomi, Kenichi; Nakako, Mamiko; Shiono, Satoru; Maeda, M. *Anal. Chim. Acta* **1988**, 212(1-2), 49-59.

65. Murakami, T.; Nakamoto, S.; Kimura, J.; Kuriyama, T.; Karube, I. *Anal. Lett.* **1986**, 19(19-20), 1973-1986.

66. Kawabe, Takeshi; Iida, Takeaki; Noguchi, Fumio; Mitamura, Takashi; Katsube, Teruaki; Tomita, K. *Nippon Kagaku Kaishi* **1987**, 9, 1719-1724.

67. Han, Xuehai; Sha, Xianzheng; Huo, J. *Shengwu Gongcheng Xuebao* **1988**, 4(2), 127-123

68. Gotoh, Masao; Tamiya, Eiichi; Seki, Atsushi; Shimizu, Isamu; Karube, I. *Anal. Lett.* 1989, 22(2), 309-302

69. Hanazato, Y.; Nakako, M.; Maeda, M.; Shiono, S. *Anal. Chim. Acta* **1987**, 193, 87-96.

70. Kimura, Jun; Saito, Atsushi; Ito, Narushi; Nakamoto, Shinya; Kuriyama, Toshihide J. *Membr. Sci.* **1989**, 43(2-3), 291-305.

71. Kimura, Jun; Ito, Narushi; Kuriyama, Toshihide; Kikuchi, Makoto; Arai, Tsunenori; Negichi, Naoki; Tomita, Yasuhiko J. *Electrochem. Soc.* **1989**, 136(6), 1744-1747.

72. Kimura, Jun; Ito, Narushi; Kuriyama, Toshihide; Kikuchi, Makoto; Atai, Tsunenori; Negishi, Naoki; Tomita, Yasuhiko; Chigira, M. *Proc.-Electrochem. Soc.* **1987**, 87(9), 327-333.

73. Vlasov, Yu. G.; Laurinavicius, V.; Tarantov, Yu. A.; Bratov, A. V.; Gureviciene, V.; Jonuska, A.; Rosga, R.; Gecis, V. *Zh. Anal. Khim.* **1989**, 44(9), 1651-1653.

74. Anzai, Junichi; Tezuka, Sachiko; Osa, Tetsuo; Nakajima, Hideki; Matsuo, T. *Chem. Pharm. Bull.* **1986**, 34(10), 4373-4376.

75. Chandler, G.K.; Dodgson, J.R.; Eddowes, M.J. *Sens. Actuators,* **1990**, B1(1-6), 433-437.

76. Sakai, Hiromitsu; Kaneki, Noriaki; Koze, Tomoyuki; Shimada, Kouji; Tanaka, Hirotoshi; Hara, H. *Denki Kagaku oyobi Kogyo Butsuri Kagaku* **1989**, 57(5), 440-441.

77. Taguchi, Hiroshi; Minaminaka, Yutaka; Ishihara, Noriyuki; Okumura, Katsuzumi; Shimabayashi, Y. *Bitamin* **1989**, 63(8), 373-376.

78. Gotoh, Masao; Tamiya, Eiichi; Momoi, Mariko; Kagawa, Yasuo; Karube, I. *Anal. Lett.* **1987**, 20(6), 857-870.

79. Shen, Youchang; Fan, Jinhua; Huang, Depei; Meng, L. *Yaoxue Xuebao* **1987**, 22(10), 785-789.

80. Iida, Takeaki; Ogura, Yumiko; Kobayashi, Hidehiko; Mitamura, Takashi; Nagata, Kazuhiko; Tomita, K. *Denki Kagaku oyobi Kogyo Butsuri Kagaku* **1988**, 56(12), 1118-1119.

81. Gotoh, Masao; Tamiya, Eiichi; Karube, I. *Nippon Kagaku Kaishi* **1987**, (11), 2214-2221.

82. Anzai, Junichi; Hashimoto, Junya; Osa, Tetsuo; Matsuo T. *Anal. Sci.* **1988**, 4(3), 247-250.

83. Shoji, Shuichi; Esashi, Masayoshi; Matsuo, T. *Sens. Actuators* **1988**, 14(2), 101-107.

84. Takasu, Nobukatsu *Kawasaki Igakkaishi* **1988**, 14(3), 336-346.

85. Kitagawa, Yasushi; Tamiya, Eiichi; Karube, I. *Anal. Lett.* **1987**, 20(1), 81-96.

86. Sakai, Hiromitsu; Kaneki, Noriaki; Koze, Tomoyuki; Shimada, Kouji; Tanaka, Hirotoshi; Hara, Hiroshi *Denki Kagaku oyobi Kogyo Butsuri Kagaku* **1989**, 57(5), 440-441.

87. Gotoh, Masao; Suzuki, Masayasu; Kubo, Izumi; Tamiya, Eiichi; Karube, I. *J. Mol. Catal.* **1989**, 53(3), 285-289

88. Oesch, Urs; Xu, Aiping; Brzozka, Zbigniew; Suter, Gabriela; Simon, W. *Chimia* **1986**, 40(10), 351-353.

89. Schasfoort, R. B. M.; Bergveld, P.; Bomer, J.; Kooyman, R. P. H.; Greve, J. *Sens. Actuators* **1989**, 17(3-4), 531-535.

90. Schasfoort, R.; Bergveld, P.; Kooyman, R.P.H.; Greve, J.; *Anal. Chim. Acta.* **1990**, 238, 323-329.

91. Pinson, L.J. *Electro-optics*, John Wiley and Sons: New York, 1985.

92. Busch, K.W.; Busch, M.A. *Multielement Detection Systems for Spectrochemical Analysis*, John Wiley and Sons: New York, 1990.

93. Adamson, A.W. *Physical Chemistry of Surfaces*, 5th ed.;John Wiley & Sons: New York, 1990; Chapter 8.

94. Petersen, J., Investigation into the Fundamental Principles of Fiber Optic Evanescent Sensors. Ph.D. Dissertation, Virginia Polytechnic Institute and State University, Blacksburg VA 24061, April 1990.

95. Hamner, V., A Fiber Optic Polarimeter for Use in Chemical Analysis. Master Thesis, Virginia Polytechnic Institute and State University, Blacksburg VA 24061, August 1990.

96. Richmond, E. Birefringent Single-arm Fiber Optic Enthalpimeter for Catalytic Reaction Monitoring. Ph.D. Dissertation, Virginia Polytechnic Institute and State University, Blacksburg VA 24061, 1990.

97. Yariv, Amnon *Introduction to Optical Electronics*, 2nd ed.; Holt, Rinehart and Winston: New York, 1976; p. 322.

98. Griffith, J.R.; O'Rear J.G. *ACS Symposium Series No. 132 Resins for Aerospace* **1980, 35-38.**

99. Hallett, M.B.; Campbell, A.K. In *Clinical and Biochemical Luminescence*, Kricka, L.J.; Carter, T., Eds.; Marcel Dekker, 1982; Chapter 6.

100. Prasher, D.; McCann, R.O.; Cormier, M.J. *Biochem. Biophys. Res. Commun.* **1985**, 126, 1259-1268.

101. Zatta, P.F.; Smith, D.F.; Cormier, M.J.; Cummings, R.D. *Anal. Biochem.* **1991**, 194, 185-191.

102. Smith, D.F. Personal communication. Letter from the University of Georgia containing data collected in their Biochemistry department laboratory.

103. Smith, D.F.; Stults, N. L.; Rivera, H.; Gehle, R. D.; Cummings, R. D.; Cormier, M.J. Personal communication of a paper to be submitted for publication from the Biochemistry department of the University of Georgia.

104. Curry, J. Ph.D Thesis, Virginia Polytechnic Institute and State University, 1985

105. Grayeski, M.L. *Anal. Chem.* **1987,** 59, 1243A-1256A.

106. Albrecht, Z. *Z. Phys. Chem.* **1928**, 136, 321.

107. Ponomarenko, A.A. *DAN* **1955**, 102, 539.

108. Babko, A.K.; Terletskaya, A.V.; Dubovenko, L.I. *Ukr. Khim. Zh.* **1966**, 32, 728.

109. Roswell, D.F.; White, E.H. *Methods in Enzymology* **1978**, 57, 409-417.

110. Seitz, R.W. *J. Phys. Chem.* **1975,** 79, 101-106.

111. Marino, D.F.; Ingle, J.D. *Anal. Chem.* **1981,** 53, 455-458.

112. Kolthoff, I. M.; Sandell, E. B. *Textbook of Quantitative Inorganic Analysis*, 3rd ed.; MacMillan Co.: New York, 1952.

113. Woolf, A.A. *Anal. Chem.* **1982, 54, 2134-2136.**

114. Themelis, D.G.; Wood, D.W.; Gordon, G. *Anal. Chim. Acta* **1989**, 225, 437-441.

115. Isacsson, U.; Wettermark, G. *Anal. Lett.* **1978**, A11, 13-25.

116. Gonzalez-Robledo, D.; Silva, M.; Perez-Bendito, D. *Anal. Chim. Acta* **1990**, 228, 123-128.

117. Choquette, S. F. Ph.D. Thesis, Virginia Polytechnic Institute and State University, 1988

118. Arney, L.H. Ph.D. Thesis, Virginia Polytechnic Institure and State University, 1989.

119. Aizawa, M.; Ikariyama, Y.; Kuno, H. *Anal. Lett.* **1984**, 17, 555-564.

120. Hooly, D. J. Ph.D. Thesis, Virginia Polytechnic Institute and State University, 1981.

121. Hooley, D.J.; Dessy, R.E. *Anal. Chem.* **1983, 55, 313.**

122. Smith, R. L.; Collins, S. D. *IEEE Transactions on Electron Devices* **1988, 35, 787-792.**

123. King, J.M.H.; DiGrazia, P.M.; Applegate, B.; Burlage, R.; Sanseverino, J.; Dunbar, P.; Larimer, F.; Sayler, G.S. *Science* **1990,** 249, 778-781.

APPENDIX

PERL PROGRAM TO RUN THE FIA SYSTEM

```
procedure inject                                    ! names procedure

clear                                               ! clear screen
input " enter up to five letters for filename " ; file$   ! get filename
file_ex$ = ".dat"                                   ! build filename
filename$ = file$ + file_ex$
input " enter description of experiment " ; header$       ! get header info
input " # of injections " ; injections%
m_d_y$ = date$
d_of_w$ = day$
h_m_s$ = time$
write m_d_y$ to filename$                           ! write header to file
write d_of_w$ to filename$
write h_m_s$ to filename$
write header$ to filename$
write injections% to filename$
display header$                                     ! display header
display "any key to begin"
x$ = inkey$                                         ! wait for a keystroke

for count% = 1 to injections%                       ! start loop
        sample_on                                   ! turn on sample pump
        display "injection #  "; count%             ! display loop status
        for wait% = 1 to 300                        ! pause for sample loop to
        next wait%                                  ! fill
        fill.on                                     ! 1st injection
        eventon                                     ! trigger LSI-11 event line
        eventoff
        fill.off
        sample_off                                  ! turn off sample pump
        com2_in                  ! procedure to get data from the LSI-11
        sample_on                                   ! turn on sample pump
        for wait% = 1 to 300
        next wait%
        inline.on                                   ! 2nd injection
        eventon
        eventoff
        inline.off
        sample_off
        com2_in
next count%

close filename$                                     ! close the file
end procedure
```

PROCEDURE *com2_in* CALLED BY THE PERL PROGRAM *inject*

```
procedure com2_in

define rc$ as serial                    ! assigns rc$ to the serial port

receive rc$                             ! receive serial info into rc$ until input
                                        ! terminator received (see manual
                                         2-10 #14 and 4-39)
write rc$ to filename$                  ! write received info to file

end procedure
```

POLYFORTH CODE FOR COLLECTING PEAK MAX AND SENDING TO PC
WHEN EVENT LINE IS TRIGGERED

```
0
1       OCTAL
2
3       ( GET POINT FROM A/D )
4
5       CODE 1GRAB 176770 CLR BEGIN 176770 TST B 0< UNTIL NEXT
6
7       ( CONVERT TO ASCII AND SEND TO PC )
8
9       CODE SIT BEGIN 176514 TST B 0< UNTIL NEXT
10      : >PC SIT 176516 C! ;
11      : >ASCII>PC ( N - )
12              (.) DUP ROT SWAP PAD SWAP CMOVE PAD SWAP OVER +
13              SWAP DO I C@ >PC LOOP 15 >PC 12 >PC ;
14      : PEAK 0 100000 0 DO 1GRAB 176772 @ MAX LOOP >ASCII>PC ;
15
```

```
0
1       ( EVENT LINE ADC TASK )
2
3       VARIABLE LTC
4       0 LTC !
5       ASSEMBLER BEGIN LTC TST 0= NOT IF LTC I) WAKE # MOV
6               THEN 200
7       100 INTERRUPT
8       : SCREEN 0TASK ;
9       : ON.R.ROBIN SCREEN ACTIVATE LTC GET
10              BEGIN STOP PEAK 0 UNTIL LTC RELEASE STOP ;
11
12
13
14
15
```

VITA

Robert St. John Smith was born in Cooperstown, N.Y. on Feburary 4, 1954. He received his elementary and secondary education in Roanoke, Va. He graduated from Patrick Henry High School in 1972. In Decemeber 1976 he received his B.S. degree, Cum Laude, in Chemistry from James Madison University. He taught at Miller School till August 1977 when he joined Merck and Co. Inc. as a Quality Control Chemist. He was a Supervisory Shift Chemist and then Chief Chemist when he left Merck to begin graduate school in the Department of Chemistry at Virginia Polytechnic Institute and State University in the summer of 1984. At Virginia Tech he was a graduate teaching assistant, academic advisor, and helped teach American Chemical Society short courses on the Electronic Laboratory. He accepted a position at St. John Fisher College in Rochester, N.Y. as an Assistant Professor of Chemistry for Fall 1991.